

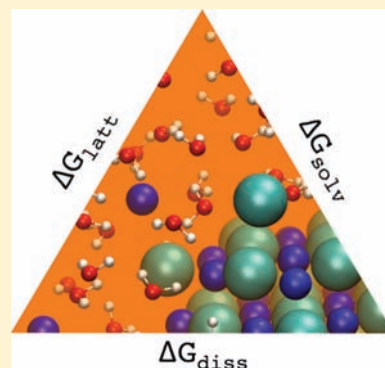
Dissolution Thermochemistry of Alkali Metal Dianion Salts (M_2X_1 , $M = Li^+$, Na^+ , and K^+ with $X = CO_3^{2-}$, SO_4^{2-} , $C_8H_8^{2-}$, and $B_{12}H_{12}^{2-}$)

Tae Bum Lee and Michael L. McKee*

Department of Chemistry and Biochemistry, Auburn University, Auburn, Alabama 36849, United States

Supporting Information

ABSTRACT: The dissolution Gibbs free energies ($\Delta G_{\text{diss}}^\circ$) of salts (M_2X_1) have been calculated by density functional theory (DFT) with Conductor-like Polarizable Continuum Model (CPCM) solvation modeling. The absolute solvation free energies of the alkali metal cations ($\Delta G_{\text{solv}}(M^+)$) come from the literature, which coincide well with half reduction potential versus SHE data. For solvation free energies of dianions ($\Delta G_{\text{solv}}(X^{2-})$), four different DFT functionals (B3LYP, PBE, BVP86, and M05-2X) were applied with three different sets of atomic radii (UFF, UAKS, and Pauling). Lattice free energies (ΔG_{latt}) of salts were determined by three different approaches: (1) volumetric, (2) a cohesive Gibbs free energy (ΔG_{coh}) plus gaseous dissociation free energy (ΔG_{gas}), and (3) the Born–Haber cycle. The G4 level of theory, electron propagator theory, and stabilization by dielectric medium were used to calculate the second electron affinity to form the dianions CO_3^{2-} and SO_4^{2-} . Only the M05-2X/Pauling combination with the three different methods for estimating ΔG_{latt} yields the expected negative dissolution free energies ($\Delta G_{\text{diss}}^\circ$) of M_2SO_4 . Salts with large dianions like $M_2C_8H_8$ and $M_2B_{12}H_{12}$ reveal the limitation of using static radii in the volumetric estimation of lattice energies. The value of ΔE_{coh} was very dependent on the DFT functional used.



INTRODUCTION

Solvation Gibbs free energies (ΔG_{solv}) contribute greatly to solubility, solution reactivity, adsorption of ionic species, and stability of biomolecules. For neutral organic species, experimental partition coefficients allow the calculation of ΔG_{solv} with 0.2 kcal/mol of uncertainty.¹ On the other hand, ΔG_{solv} of individual cations or anions are not directly available by experiment and in many cases the uncertainty is substantial (4 to 5 kcal/mol).¹ Alkali metal cations, which play a key role in biology, have widely varying reported values of ΔG_{solv} (Table 1).² The absolute ΔG_{solv} of Li^+ , Na^+ , and K^+ vary from -104.1 to -144.3 kcal/mol, -76.8 to -116.5 kcal/mol, and -59.6 to -85.4 kcal/mol, respectively.³ Latimer⁴ estimated ΔG_{solv} of alkali metal cations using a thermodynamic cycle which included sublimation energy, ionization energy, and reduction potential. However, the entropy of solids, electron/ion convention, and standard reduction potential were not accurately known at that time. Tissandier et al.^{3d} presented a cluster-pair approximation to get the absolute ΔG_{solv} of alkali metal cations. Kelly et al.³ⁱ applied the same method to determine the absolute ΔG_{solv} of alkali metal cations with the electron convention/Fermi-Dirac statistics. Donald and Williams^{3j} performed an even more comprehensive cluster-pair approximation and reported slightly modified ΔG_{solv} of alkali metal cations based on -263.4 kcal/mol of $\Delta G_{\text{solv}}(H^+)$ at 1 atm standard state (Table 1).

The CPCM (Conductor-like Polarizable Continuum Model)⁵ is combined with ab initio computations to determine ΔG_{solv} of neutral and ionic species. In a benchmark study of CPCM,

Takano and Houk⁶ found that the mean absolute deviations of aqueous ΔG_{solv} for ionic species varied between 2.73 and 9.30 kcal/mol depending on the choice of the cavity set. The Pauling cavity set had the smallest deviation (2.73 kcal/mol) for ionic species while the same cavity set showed 3.49 kcal/mol of deviation for neutral species. Takano and Houk⁶ recommended the UAKS cavity set for the prediction of pK_{a1} since it had the smallest deviation for neutral species (1.35 kcal/mol) and a small deviation for anions (3.21 kcal/mol). However, Chipman⁷ reported that no single electronic isodensity contour value for solute cavity led to acceptable values of ΔG_{solv} for anions in his test sets. Król et al.⁸ suggested that the Pauling cavity set was best for pK_a predictions of polyprotic acids. Fernández et al.⁹ found that the Pauling cavity set was better than the UAKS cavity set for the pK_a calculation of ammonia oxide ($^+NH_3O^-$). We found the Pauling cavity set with M05-2X is the most suitable to the $\Delta G_{\text{aq2}}/pK_{a2}$ prediction in aqueous media.¹⁰ The CPCM method with a proper choice of a cavity set can yield solvation free energies (ΔG_{solv}) of anions within about ± 5 kcal/mol of experiment.¹

Many ab initio computations based on periodic or extended cluster models have been performed for organic crystal lattice energy.¹¹ Dispersion interactions, which are the main intermolecular contribution to the organic crystal lattice energy, are not described properly with traditional density functional theory (DFT) methods. The Grimme group^{11b,12} have developed an

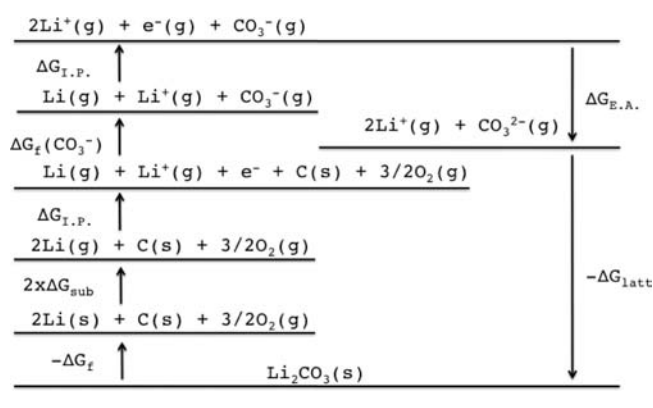
Received: May 31, 2011

Published: October 24, 2011

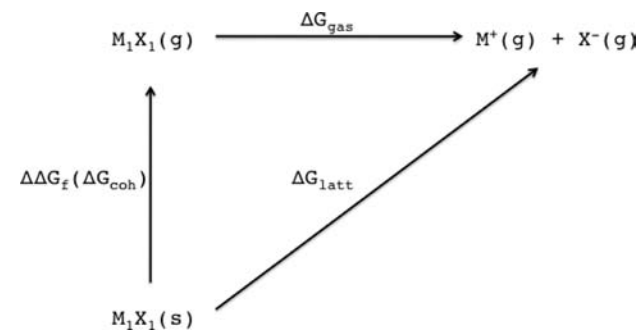
Table 1. Absolute Hydration Free Energies (ΔG_{solv} , kcal/mol) of Alkali Metal Cations (Li^+ , Na^+ , K^+) in Literature^a

reference	absolute hydration free energy (ΔG_{solv})		
	Li^+	Na^+	K^+
3o	-122.1	-98.4	-80.6
3n	-122.1	-98.2	-80.6
3a	-123.5	-98.6	-80.8
3p	-113.5	-87.2	-70.5
3c ^b	-144.3	-116.5	
3d	-126.5	-101.3	-84.1
3e	-115.4	-96.3	-79.6
3f	-126.0		
3g	-124.9	-99.7	-82.5
3h	-118.6	-94.2	
3m			-68.6
3i	-126.5	-101.3	-84.1
3j ^b	-120.8	-92.3	-75.5
3q	-123.1	-96.6	-79.4
3k	-111.8	-86.8	-68.8
3k	-104.1	-76.8	-59.6
3k	-112.8	-87.5	-65.0
3l	-127.8	-102.6	-85.4
3r	-120.5	-96.3	-78.6
this work ^c	-126.6	-101.1	-83.8

^aThe standard state of 1 atm for gas and 1 M for aqueous solution. The reported values with 1 M standard state for gas and solution are converted to the values with the standard state of 1 atm of gas and 1 M for aqueous solution using a +1.89 kcal/mol correction. ^bThe standard state information is not shown clearly. ^cThe SHE 4.281 eV is applied. See Scheme 4 for details. The values used (in bold) for $\Delta G_{\text{solv}}(\text{M}^+)$ are from ref 3i.

Scheme 1. Born–Haber Cycle for Li_2CO_3 

empirically parametrized dispersion correction which is implemented in several packages for periodic systems. For the Born–Haber cycle of M_2CO_3 and M_2SO_4 ($\text{M} = \text{Li}^+$, Na^+ , and K^+), determining the second electron affinity is also a challenge (Scheme 1).¹³ Most thermodynamic properties are well-known from the literature or can be computed by established methods (Scheme 1). On the other hand, small dianions such as CO_3^{2-} and SO_4^{2-} are known to be stable in water but unstable or metastable in the gas phase because of the unbound nature of the

Scheme 2. Lattice Free Energy of a Crystal by the Sum of Free Energy Difference ($\Delta\Delta G = \Delta\Delta H_f - T\Delta S$) between Gas and Solid Followed by Gaseous Dissociation Free Energy (ΔG_{gas})

second electron.^{10,14} Many approaches have been presented to calculate the second electron affinity (negative affinity) using chemical hardness,¹⁵ an anion bound by potential wall,¹⁶ and the stabilization exerted by a polar solvent.¹⁷ Jensen¹⁸ reported that the lack of long-range dispersion in the exchange-correlation DFT functional led to poor performance for calculating electron affinities. The electron affinities (negative electron affinity, $-\Delta H_{0K}$) of CO_3^{2-} and SO_4^{2-} are known to be -87.6 kcal/mol and -37.0 kcal/mol, respectively from the literature.¹⁹ The electron affinity of SO_4^{2-} by the MP2/CBS method was -25.4 kcal/mol²⁰ while the Simons group²¹ reported SO_4^{2-} was vertically unstable by 25.8 kcal/mol.

Over the past 10 years, the Jenkins group²² developed a volumetric approach for the lattice energy of ionic crystals including an empirical formula for entropy estimation. Several studies have used this volumetric approach to determine the lattice energy of ionic crystals because the equation is very easy to apply.²³ The lattice enthalpies of M_2CO_3 and M_2SO_4 ($\text{M} = \text{Li}^+$, Na^+ , and K^+) in the literature are available based on this volumetric approach as well as the Born–Fajans–Haber cycle.²⁴ In fact, we consider the volumetric approach more reliable because the heat of formation for $\text{CO}_3^{2-}(\text{g})$ and $\text{SO}_4^{2-}(\text{g})$ are uncertain.²⁴ However, the choice of ionic volume is critical to determine the lattice energy. For $\text{K}_2\text{B}_{12}\text{Cl}_{12}$, 0.010 nm³ for the K^+ volume^{23d} gives 250.7 kcal/mol of lattice energy while 0.0277 nm³ by a recent study^{22h} gives 294.6 kcal/mol of lattice energy, a difference of 43.9 kcal/mol.

If the formation Gibbs free energy differences ($\Delta\Delta G_f = \Delta\Delta H_f - T\Delta S$) between gas and solid are available, a thermodynamic triangle can be constructed to estimate ΔG_{latt} (Scheme 2). Calculating the gaseous dissociation energy (ΔG_{gas}) of an ionic molecule by ab initio quantum chemistry is straightforward. In addition, many papers are beginning to appear on the calculation of ΔH_f in the solid.²⁵ We also define a cohesive free energy of the crystal (ΔG_{coh}), which can replace $\Delta\Delta G_f$ in Scheme 2. With the optimized geometry of the gaseous ionic molecule and the optimized crystal structure, the cohesion energy of the crystal can be estimated by computation.

We set up a thermodynamic cycle for the dissolution of alkali metal cations (Li^+ , Na^+ , and K^+) with several dianions (CO_3^{2-} , SO_4^{2-} , $\text{C}_8\text{H}_8^{2-}$, and $\text{B}_{12}\text{H}_{12}^{2-}$) in Scheme 3. At equilibrium, ΔG_{diss} is always 0 while $\Delta G_{\text{diss}}^\circ$ is given by $-RT \ln K_{\text{sp}}$ ($\Delta G_{\text{diss}} = \Delta G_{\text{diss}}^\circ + RT \ln K_{\text{sp}}$, where K_{sp} is solubility constant). With ΔH_f for aqueous ions and solids and entropies for aqueous ions and salts, $\Delta G_{\text{diss}}^\circ$ of M_2CO_3 ($\text{M} = \text{Li}^+$, Na^+ , and K^+) in infinitely

Scheme 3. Thermodynamic Cycle for the Dissolution of M_2X_1 (M_2X_1 , $M = Li^+$, Na^+ , and K^+ with $X = CO_3^{2-}$, SO_4^{2-} , $C_8H_8^{2-}$, and $B_{12}H_{12}^{2-}$) Salts

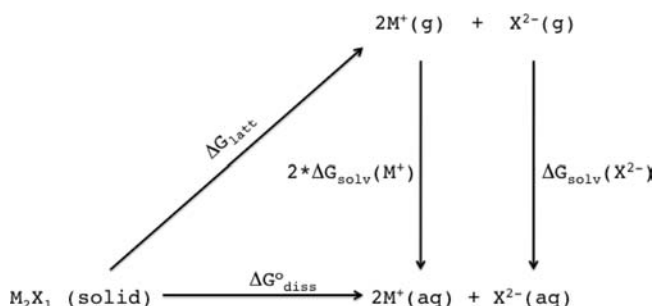


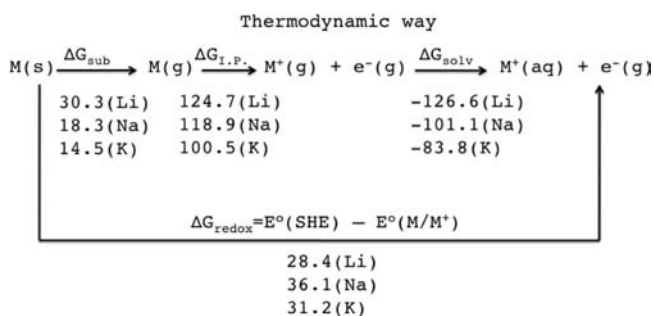
Table 2. Experimental Dissolution Enthalpies ($\Delta H^\circ_{\text{diss}}$) and Free Energies ($\Delta G^\circ_{\text{diss}}$) (kcal/mol) of M_2CO_3 ($M = Li^+$, Na^+ , and K^+), M_2SO_4 ($M = Li^+$, Na^+ , and K^+), and $M_2B_{12}H_{12}$ ($M = Li^+$, Na^+ , K^+ , Rb^+ , and Cs^+)

dissolution reaction	$\Delta H^\circ_{\text{diss}}{}^a$	$\Delta G^\circ_{\text{diss}}{}^b$	$\Delta G^\circ_{\text{diss}}{}^c$
$Li_2CO_3(s) \rightarrow 2Li^+(aq) + CO_3^{2-}(aq)$	-4.3	4.3	2.2
$Na_2CO_3(s) \rightarrow 2Na^+(aq) + CO_3^{2-}(aq)$	-6.4	-1.1	-2.1
$K_2CO_3(s) \rightarrow 2K^+(aq) + CO_3^{2-}(aq)$	-7.6	-7.1	-4.5
$Li_2SO_4(s) \rightarrow 2Li^+(aq) + SO_4^{2-}(aq)$	-7.2	-2.3	-2.4(-0.1) ^d
$Na_2SO_4(s) \rightarrow 2Na^+(aq) + SO_4^{2-}(aq)$	-0.5	0.4	-1.4(1.7) ^d
$K_2SO_4(s) \rightarrow 2K^+(aq) + SO_4^{2-}(aq)$	5.6	2.0	-0.2(2.4) ^d
$Li_2B_{12}H_{12}(s) \rightarrow 2Li^+(aq) + B_{12}H_{12}^{2-}(aq)$			-2.7 ^e
$Na_2B_{12}H_{12}(s) \rightarrow 2Na^+(aq) + B_{12}H_{12}^{2-}(aq)$			-2.6 ^e
$K_2B_{12}H_{12}(s) \rightarrow 2K^+(aq) + B_{12}H_{12}^{2-}(aq)$			-1.9 ^e
$Rb_2B_{12}H_{12}(s) \rightarrow 2Rb^+(aq) + B_{12}H_{12}^{2-}(aq)$			1.4 ^e
$Cs_2B_{12}H_{12}(s) \rightarrow 2Cs^+(aq) + B_{12}H_{12}^{2-}(aq)$			4.0 ^e

^aThe $\Delta H^\circ_{\text{diss}}$ is taken as the difference in the aqueous heat of formation (standard state is hypothetical ideal solution with molality $m = 1$ mol/kg) in reference 24b and the solid state heat of formation in the NIST webbook. ^bFree energy of the solid (ΔG) is taken as the heat of formation for the solid state (ΔH_f) plus the entropy term ($-T\Delta S$) while the entropy for the aqueous ion comes from reference 24b. ^cThe $\Delta G^\circ_{\text{diss}}$ comes from the K_{sp} ($\Delta G = -RT \ln K_{\text{sp}}$) with concentration from solubility data. ^dThe values in parentheses are determined using solubility data with activity coefficient (Guendouzi, M. E.; Mounir, A.; Dinane, A. *J. Chem. Thermodynamics* **2003**, *35*, 209–220). For solubility of Na_2SO_4 , a value of 20 g/100 g water applied for 25 °C solubility. ^eThe $\Delta G^\circ_{\text{diss}}$ comes from the K_{sp} ($\Delta G = -RT \ln K_{\text{sp}}$) with concentration (activity coefficients are not used) from solubility data in reference 27.

dilute solutions are between -7.1 (K_2CO_3) to 4.3 kcal/mol (Li_2CO_3) while $\Delta G^\circ_{\text{diss}}$ of M_2SO_4 ($M = Li^+$, Na^+ , and K^+) are between -2.3 (Li_2SO_4) to 2.0 kcal/mol (K_2SO_4) (Table 2).^{24b} The solubility of M_2CO_3 , M_2SO_4 , and $M_2B_{12}H_{12}$ ($M = Li^+$, Na^+ , and K^+) varies greatly while the $\Delta G^\circ_{\text{diss}}$ by $-RT \ln K_{\text{sp}}$ is within ± 5 kcal/mol of 0 (Table 2 and Supporting Information, Table S2).²⁶ All $M_2B_{12}H_{12}$ salts ($M = Li^+$, Na^+ , and K^+) are known to be very soluble in water and stable in dilute acids, but the solubility decreases sharply from lithium to the cesium salt.^{23c,27,28} The value of $\Delta G^\circ_{\text{diss}}$ can be determined more accurately using activity coefficients rather than concentrations but the adjusted $\Delta G^\circ_{\text{diss}}$

Scheme 4. Thermodynamic Cycle for the Evaluation of Absolute ΔG_{solv} of M ($M = Li^+$, Na^+ , and K^+)^a



^a ΔG_{sub} , $\Delta G_{\text{I.P.}}$, ΔG_{redox} and ΔG_{solv} are in kcal/mol.

for M_2SO_4 ($M = Li^+$, Na^+ , and K^+) still remains within ± 5 kcal/mol of 0 (Table 2). The maximum difference in $\Delta G^\circ_{\text{diss}}$ for M_2SO_4 ($M = Li^+$, Na^+ , and K^+) between using concentrations and activities is 2.6 kcal/mol (Table 2). In this work, we determine $\Delta G^\circ_{\text{diss}}$ through ab initio computation for the lattice free energy (ΔG_{latt}) and solvation free energy (ΔG_{solv}). It is well-known that solubilities of salts can be rationalized by considering lattice and hydration enthalpies. Our intention is to combine experiment and theory to evaluate dissolution free energies and to determine a methodology that gives results most consistent with experiment.

COMPUTATIONAL DETAILS

The B3LYP, PBE, BVP86, and M05-2X²⁹ DFT functionals are applied with the aug-cc-pVTZ basis set to calculate $\Delta G_{\text{gas}}(M_2X_1(g) \rightarrow 2M^+(g) + X^{2-}(g))$. Zero-point energies, heat capacity corrections, and $T\Delta S$ contributions are combined with single-point energies at the same level to yield free energies at 298 K. For potassium-containing systems, the 6-311++G(3df,2pd) basis set was used. The ΔG_{gas} values were applied in Scheme 2 for the estimation of ΔG_{latt} .

The conductor-like polarizable continuum model (CPCM)⁵ was applied with the dielectric constant of water ($\epsilon = 78.39$) and the SCFVAC Gaussian03 keyword on gas-phase optimized geometries to compute ΔG_{solv} . For atomic radii in CPCM, we tested three cavity models (UFF, UAKS, and Pauling).¹⁰ No symmetry restrictions were made on the cavity, and the cavity surface was fit with tesserae of average area 0.1 Å². Geometries, gaseous free energies, and solvation free energies for the three cavity models were obtained using Gaussian03.³⁰ Since the $\Delta G_{\text{solv}}(X^{2-})$ values by ab initio calculations are based on the standard state of 1 atm (24.47 L/mol), we used a factor of +1.89 kcal/mol to convert to the standard state of 1 M (1 L/mol).

In Scheme 4, we evaluate ΔG_{solv} of Li^+ , Na^+ , and K^+ using the standard reduction potentials of alkali metal cations,³¹ including correction for electron/ion convention³² and standard state conversion.³³ The determination of the absolute ΔG_{solv} of alkali metal cations depends on the choice of standard hydrogen electrode (SHE) potential. Reiss and Heller³⁴ reported 4.43 eV while Donald et al.³⁵ suggested 4.2 ± 0.4 eV and proposed 4.11 eV using nanodrops in gas phase. However, Isse and Gennaro³⁶ reported 4.281 eV using the real potential, $\alpha_{\text{aq}}(H^+)$ ($\alpha_{\text{aq}}(H^+) = \Delta G_{\text{aq}}(H^+) + F\chi^{\text{aq}}$, where χ^{aq} is the surface potential of water). In the electrochemical approach, the difference between $E^\circ(\text{SHE})$ and the half reduction potential of each alkali metal cation ($E^\circ(M/M^+)$) determines the free energy change (ΔG_{redox}) of $M(s) \rightarrow M^+(aq) + e^-(g)$ (Scheme 4). The solvation free energy (ΔG_{solv}) comes from ($\Delta G_{\text{redox}} - \Delta G_{\text{sub}} - \Delta G_{\text{I.P.}}$). The difference of ΔH_f between gas and solid phase followed by entropy change is ΔG_{sub} . The ionization potential of alkali metal atom (ΔH_{0K}) in the ion convention plus

entropy change between atom and cation is ΔG_{LP} , at 298 K since the heat capacity corrections of the monocation and monoatom are identical and cancel out. Enthalpies, entropies, and ionization potentials (ion-convention, Fermi-Dirac statistics) for each step are taken from the NIST chemistry webbook.³⁷ If 4.281 eV is used for SHE (1 atm standard state), the absolute $\Delta G_{\text{solv}}(\text{M}^+)$ ($\text{M}^+ = \text{Li}^+, \text{Na}^+, \text{and K}^+$) become $-126.6, -101.1, \text{ and } -83.8$ kcal/mol, respectively. These values are very similar to the $\Delta G_{\text{solv}}(\text{M}^+)$ ($\text{M}^+ = \text{Li}^+, \text{Na}^+, \text{ and K}^+$) at 1 atm standard state suggested by three different cluster-pair approximation studies (Table 1 and Scheme 4).^{3d,4l} Values that deviate by more than ± 5 kcal/mol from the cluster-pair approximation studies should be carefully reevaluated. We used the values of $\Delta G_{\text{solv}}(\text{M}^+)$ ($\text{M}^+ = \text{Li}^+ (-126.5), \text{Na}^+ (-101.3), \text{ and K}^+ (-84.1)$ kcal/mol) reported by Kelly et al.³ⁱ after correcting to our standard state conversion of 1 M for solution (+1.89 kcal/mol).

The hydrolysis of SO_4^{2-} ($\text{H}_2\text{O}(\text{l}) + \text{SO}_4^{2-}(\text{aq}) \rightarrow \text{HSO}_4^-(\text{aq}) + \text{OH}^-(\text{aq})$) is non-spontaneous at pH 7 ($\Delta G = 16.4$ kcal/mol, see Supporting Information for details) which indicates that the anionic species in the dissolution of $\text{M}_2\text{SO}_4(\text{s})$ will be SO_4^{2-} rather than HSO_4^- . Likewise, the hydrolysis of CO_3^{2-} ($\text{H}_2\text{O}(\text{l}) + \text{CO}_3^{2-}(\text{aq}) \rightarrow \text{HCO}_3^-(\text{aq}) + \text{OH}^-(\text{aq})$) is non-spontaneous at pH 7 ($\Delta G = 5.0$ kcal/mol) which indicates that the anionic species in the dissolution of $\text{M}_2\text{CO}_3(\text{s})$ will be CO_3^{2-} rather than HCO_3^- . For $\text{M}_2\text{C}_8\text{H}_8$ ($\text{M} = \text{Li}^+, \text{Na}^+, \text{ and K}^+$), $\text{M}_2\text{C}_8\text{H}_8(\text{s}) \rightarrow 2\text{M}^+(\text{aq}) + \text{C}_8\text{H}_8^{2-}(\text{aq})$ is not the process observed because of the further reaction and formation of insoluble $\text{C}_8\text{H}_{10}(\text{l})$ (1,3,5-cyclooctatriene) on top of water.³⁸ The dianion $\text{C}_8\text{H}_8^{2-}$ undergoes hydrolysis to form $\text{C}_8\text{H}_{10}(\text{l})$. The experimental aqueous heat of reaction (ΔH_{rxn}) for $\text{M}_2\text{C}_8\text{H}_8(\text{s}) + 2\text{H}_2\text{O}(\text{l}) \rightarrow 2\text{M}^+(\text{aq}) + 2\text{OH}^-(\text{aq}) + \text{C}_8\text{H}_{10}(\text{l})$ ($\text{M} = \text{Li}^+, \text{Na}^+, \text{ and K}^+$) was found to be $-37.3, -33.3, \text{ and } -28.8$ kcal/mol, respectively.^{38,39} The calculated ΔG for $\text{C}_8\text{H}_8^{2-}$ hydrolysis at pH 7 ($2\text{H}_2\text{O}(\text{l}) + \text{C}_8\text{H}_8^{2-}(\text{aq}) \rightarrow \text{C}_8\text{H}_{10}(\text{l}) + 2\text{OH}^-(\text{aq})$) is -34.7 kcal/mol (further details given below). The dianion $\text{B}_{12}\text{H}_{12}^{2-}$ does not undergo hydrolysis.

In the volumetric approach with the Jenkins formula,^{22d-f} lattice energies (U_{POT}), enthalpy corrections, and solid entropies were calculated by the sum of cation and anion thermodynamic volumes (V_{m}) (eqs 1, 2, and 3).

$$U_{\text{POT}} = 2I(\alpha V_{\text{m}}^{1/3} + \beta) \quad (1)$$

$$\Delta H_{\text{L}} = U_{\text{POT}} + [p(n_{\text{M}}/2 - 2) + q(n_{\text{X}}/2 - 2)]RT \quad (2)$$

$$S_{298}^{\circ} = 325V_{\text{m}} + 3.6 \quad (3)$$

For M_2X_1 crystal systems, $\alpha, \beta,$ and I are 39.55 nm \cdot kcal/mol, -7.12 kcal/mol, constant 3 while $p, q, n_{\text{M}},$ and n_{X} are constants 2, 1, 3, and 6, respectively.^{22d}

The ionic volumes of $\text{Li}^+, \text{Na}^+, \text{ and K}^+$ are 0.0067, 0.0158, and 0.0277 nm 3 , respectively, while ionic volumes of CO_3^{2-} and SO_4^{2-} are 0.0426 and 0.0611 nm 3 , respectively.^{22h} The ionic volume of $\text{C}_8\text{H}_8^{2-}$ and $\text{B}_{12}\text{H}_{12}^{2-}$ are 0.1868 and 0.2950 nm 3 , as determined by ab initio computation (0.001 e/bohr 3 density envelop, using Gaussian03³⁰ keyword "VOLUME"). The geometries and electron densities of $\text{C}_8\text{H}_8^{2-}$ and $\text{B}_{12}\text{H}_{12}^{2-}$ are taken from the ab initio results by M05-2X/6-311++G(3df,2pd) and M05-2X/aug-cc-pVTZ, respectively.

For the Born-Haber cycle, we use enthalpies from the NIST chemistry webbook followed by entropy corrections to form free energies.³⁷ Literature values of ΔH_{f} for the monoanions ($\text{CO}_3^-, \text{SO}_4^-, \text{ and C}_8\text{H}_8^-$) were combined with entropies at the G4 level of theory⁴⁰ to form free energies. If ΔH_{f} was not available in the literature, we applied an isodesmic equation at the G4 level of theory.⁴¹ For the electron affinity of a monoanion, an adiabatic energy difference between the monoanion radical and dianion was calculated at the G4 level of theory. A "bound" electron attachment was computed for $\text{CO}_3^-, \text{SO}_4^-, \text{ and C}_8\text{H}_8^-$ at the CCSD(T)/G4 level of theory by using a series of dielectric

medium calculations. Propagator theory (Outer Valence Green's Function),⁴² an alternative method to calculate electron attachment or detachment energies, was used to compare with CCSD(T)/G4 calculations. The OVGF(P3)/aug-cc-pVQZ level of theory was applied to CO_3^{2-} and SO_4^{2-} while the OVGF(P3)/aug-cc-pVTZ level of theory was applied to $\text{C}_8\text{H}_8^{2-}$ with geometry and ZPE corrections taken from B3LYP/GTbas3 (G4 level of theory). We used the β -LUMO orbital energy of the monoanion in the dianion geometry by OVGF(P3) for the adiabatic electron attachment.

For ΔG_{latt} by Scheme 2, we applied an atomization scheme⁴³ to determine the gaseous ΔH_{f} of M_2CO_3 ($\text{M} = \text{Li}^+, \text{Na}^+, \text{ and K}^+$) since the value was not available in the NIST webbook. We found the most stable geometry of gaseous Li_2CO_3 to be C_{2v} symmetry⁴⁴ and used that point group to determine the geometry of Na_2CO_3 and K_2CO_3 . If the crystal structure was available, we used periodic ab initio computations to determine the ΔE_{coh} , the energy to release one molecular unit from one unit cell of the ionic crystal (eq 4).

$$\Delta E_{\text{coh}} = E_{\text{unit}} - E_{\text{bulk}}/N_{\text{unit}} \quad (4)$$

The energy of one molecular unit is E_{unit} while E_{bulk} is the total energy of one crystal unit cell and N_{unit} is the number of molecular units in a crystal unit cell. We performed total energy calculations of a unit cell with a $4 \times 4 \times 4$ K-point grid. The BLYP, PBE, PW91, PZ functionals and the PBE-D (PBE functional with Grimme's dispersion correction) were applied. All pseudopotentials in this study are ultrasoft or norm-conserving (see detail in Supporting Information, Table S13). The ΔE_{coh} calculations for M_1Cl ($\text{M} = \text{Li}^+, \text{Na}^+, \text{ and K}^+$) were performed for comparison. The crystal structure of LiCl is the α -form, which is exclusively available above -30 °C.⁴⁵ We selected crystal structures of M_2SO_4 ($\text{M} = \text{Li}^+, \text{Na}^+, \text{ and K}^+$) at ambient conditions.⁴⁶ The ΔE_{coh} calculations for M_2CO_3 ($\text{M} = \text{Li}^+, \text{Na}^+, \text{ and K}^+$) were not performed since the Na_2CO_3 crystal is disordered⁴⁷ and the K_2CO_3 molecular geometry in the unit cell is not well reproduced. The anhydrous crystal structure of $\text{M}_2\text{C}_8\text{H}_8$ ($\text{M} = \text{Li}^+, \text{Na}^+, \text{ and K}^+$) is not known but $\text{K}_2\text{C}_8\text{H}_8 \cdot \text{diglyme}$ and $\text{K}_2\text{C}_8\text{H}_8 \cdot (\text{THF})_3$ are available.⁴⁸ The crystal structures of $\text{M}_2\text{B}_{12}\text{H}_{12}$ ($\text{M} = \text{Li}^+, \text{Na}^+, \text{ and K}^+$), which have recently been solved, were subjected to ΔE_{coh} calculations.⁴⁹ For the molecular unit in the gas phase, the gaseous geometry of M_2X_1 was obtained in a $20 \times 20 \times 20$ Å box with fixed cell parameters. The geometry optimization was performed with an energy cutoff of 40 Ry. All periodic boundary calculations were done using the Quantum-Espresso Package 4.2.1.⁵⁰ For the zero-point energy (ZPE) and entropy ($T\Delta S$) contributions to the free energy of the solid, we used the PM6 semiempirical method⁵¹ for the cluster model of the crystal unit cell. Sherwood⁵² summarizes the missing terms when we apply gas phase vibration spectra to the solid. A number of entirely new bands, which are in the low frequency region (<800 cm $^{-1}$) by external vibration, are missed in this approach. For metal/metal oxide (Ru/RuO_2 or Ir/IrO_2), ab initio computation for the solid ignored the ZPE and entropy correction since the contribution for metal/metal oxide was less than 2.3 kcal/mol.⁵³ However, ZPE contribution (ΔE_{ZPE}) for the $\Delta\Delta G_{\text{f}}(\Delta G_{\text{coh}})$ in Scheme 2 by PM6 is usually 1 or 2 kcal/mol while the entropy correction by the $T\Delta S$ term is about 10 kcal/mol (Supporting Information, Table S3). For the cohesive free energy (ΔG_{coh}) at 298.15 K, the thermal correction energy between solid and gas should be applied ($2RT$).⁵⁴ However, given the large uncertainty in the calculation of ΔG_{coh} , the small correction is omitted from our calculations.^{22g,54} The lattice free energy notation $\Delta G_{\text{latt-1}}, \Delta G_{\text{latt-2}}, \text{ and } \Delta G_{\text{latt-3}}$ represent ΔG_{latt} (1) by the Jenkins formula (eqs 1–3), (2) by ($\Delta\Delta G + \Delta G_{\text{gas}}$) (Scheme 2), and (3) by the Born-Haber cycle (Scheme 1), respectively.

RESULTS AND DISCUSSION

The sum of $\Delta G_{\text{solv}}(\text{M}^+\text{X}^-)$ and ΔG_{latt} ($\Delta G_{\text{latt-1}}, \Delta G_{\text{latt-2}}, \text{ or } \Delta G_{\text{latt-3}}$) give the free energies of dissolution ($\Delta G_{\text{diss}}^{\circ}$) for M_1X_1

Table 3. Dissolution Free Energy ($\Delta G_{\text{diss}}^{\circ}$) by $\Delta G_{\text{latt-1}}$ (Jenkins Formula), $\Delta G_{\text{latt-2}}$ ($\Delta\Delta G + \Delta G_{\text{gas}}$), and $\Delta G_{\text{latt-3}}$ (Born–Haber cycle) for M_1X_1 ($M = \text{Li}^+$, Na^+ , and K^+ ; $X = \text{F}^-$, Cl^- , Br^- , and I^-) Salts^a

M_1X_1	$\Delta G_{\text{latt-3}}^b$ (Born–Haber)	$\Delta G_{\text{diss}}^{\circ}$ ($\Delta G_{\text{latt-1}}^{\text{c,e,h}}$)	$\Delta G_{\text{diss}}^{\circ}$ ($\Delta G_{\text{latt-2}}^{\text{d,f}}$)	$\Delta G_{\text{diss}}^{\circ}$ ($\Delta G_{\text{latt-3}}^g$)
LiF	233.1	−18.1(−22.2)	2.7(−1.4)	4.1(0.0)
LiCl	189.5	−22.4(−12.6)	−10.8(−1.0)	−9.8(0.0)
LiBr	179.6	−24.7(−11.4)	−14.9(−1.6)	−13.3(0.0)
LiI	166.5	−28.3(−10.9)		−17.4(0.0)
NaF	204.9	−16.2(−17.4)	−0.5(−1.6)	1.2(0.0)
NaCl	171.7	−9.4(−7.1)	−3.3(−1.0)	−2.3(0.0)
NaBr	163.7	−9.5(−5.6)	−4.4(−0.5)	−3.9(0.0)
NaI	152.3	−10.5(−4.2)		−6.3(0.0)
KF ⁱ	181.2	−17.6(−12.1)	−3.8(1.6)	−5.5(0.0)
KCl ⁱ	155.3	−3.6(−2.1)	−2.2(−0.7)	−1.5(0.0)
KBr ⁱ	148.8	−2.1(−0.5)	−2.9(−1.3)	−1.6(0.0)
KI ⁱ	139.2	−0.9(1.4)		−2.3(0.0)

^a The solvation free energy of salt ($\Delta G_{\text{solv}}(M^+X^-)$) comes from ref 31. For 1 atm standard state, 3.78 kcal/mol (1.89×2) of correction should be applied to final $\Delta G_{\text{diss}}^{\circ}$. ^b All experimental values for Born–Haber cycle are taken from the NIST chemistry webbook. ^c Ion volumes are taken from ref 22h and entropy comes from NIST chemistry webbook. ^d Free energy differences ($\Delta\Delta G$) are taken from NIST chemistry webbook while ΔG_{gas} values are taken from the average of four different DFT functionals. ^e Value in parentheses is the difference between $\Delta G_{\text{latt-1}}$ (Jenkins formula) and $\Delta G_{\text{latt-3}}$ (Born–Haber). ^f Value in parentheses is the difference between $\Delta G_{\text{latt-2}}$ ($\Delta\Delta G + \Delta G_{\text{gas}}$) and $\Delta G_{\text{latt-3}}$ (Born–Haber). ^g Value in parentheses is the difference between $\Delta G_{\text{latt-3}}$ (Born–Haber) and $\Delta G_{\text{latt-3}}$ (Born–Haber). ^h The equations of the Jenkins formula for M_1X_1 salts are $U_{\text{POT}} = 2(28.0V_m + 12.4)$, $\Delta H_L = U_{\text{POT}} - RT$ and solid entropies of M_1X_1 salts are taken from NIST webbook. ⁱ ΔG_{gas} is computed at the DFT/6-311++G(3df,2pd) level for potassium-containing molecules.

($M = \text{Li}^+$, Na^+ , K^+ with $X = \text{F}^-$, Cl^- , Br^- , and I^-) salts (Table 3). The $\Delta G_{\text{solv}}(M^+X^-)$ and $\Delta G_{\text{latt-3}}$ combination is the most reliable method of computing $\Delta G_{\text{diss}}^{\circ}$ for M_1X_1 salt systems since it depends only on reliable experimental data. However, the $\Delta G_{\text{solv}}(M^+X^-)$ and $\Delta G_{\text{latt-2}}$ combination also give $\Delta G_{\text{diss}}^{\circ}$ free energies which are in very close agreement (± 1.6 kcal/mol maximum deviation from $\Delta G_{\text{latt-3}}$). However, the Jenkins formula substantially underestimates all ΔG_{latt} values for M_1X_1 salts except for KCl, KBr, and KI (Table 3). With the same cation, smaller anions produce larger errors, while smaller cations produce larger errors with the same anion. For the less soluble salts, LiF and NaF, the underestimation of $\Delta G_{\text{latt-1}}$ is substantial (−22.2 and −17.4 kcal/mol, respectively). The $\Delta G_{\text{latt-1}}$ values are determined with the eqs 1–3 and radii from the Jenkins group.²² However, different formula and radii have been suggested in the past, some of which have yielded more accurate values of ΔG_{latt} for M_1X_1 .^{22a,b,h}

Table 4 summarizes $\Delta G_{\text{solv}}(X^{2-})$ in an aqueous solution by the CPCM method with three different cavity sets. In the same cavity set, the M05–2X functional always gives the most negative $\Delta G_{\text{solv}}(X^{2-})$ and the Pauling cavity set always gives the most negative $\Delta G_{\text{solv}}(X^{2-})$ among the three cavity radii sets except for $\Delta G_{\text{solv}}(\text{B}_{12}\text{H}_{12}^{2-})$. The UFF cavity set gives the smallest $\Delta G_{\text{solv}}(X^{2-})$ for CO_3^{2-} and SO_4^{2-} while the UAKS cavity set gives the smallest $\Delta G_{\text{solv}}(X^{2-})$ for $\text{C}_8\text{H}_8^{2-}$ and $\text{B}_{12}\text{H}_{12}^{2-}$ (Table 4). The differences ($\Delta G_{\text{solv}}(\text{M05–2X}/\text{Pauling}) - \Delta G_{\text{solv}}(\text{M05–2X}/\text{UFF})$) become smaller as the size of the dianion increases (−20.5, −17.5, −7.0, and 1.0 kcal/mol for CO_3^{2-} , SO_4^{2-} , $\text{C}_8\text{H}_8^{2-}$, and $\text{B}_{12}\text{H}_{12}^{2-}$). For $\Delta G_{\text{solv}}(X^{2-})$, the UFF and UAKS cavity sets show a strong dependence on size of the dianion but not the shape because all dianions are highly symmetric (CO_3^{2-} in D_{3h} , SO_4^{2-} in T_d , $\text{C}_8\text{H}_8^{2-}$ in D_{8h}) or even icosahedral ($\text{B}_{12}\text{H}_{12}^{2-}$ in I_h).

The accuracy of ΔG_{latt} (relative to $\Delta G_{\text{latt-3}}$) is presented in Figure 1 for $M_2\text{CO}_3$ ($M = \text{Li}^+$, Na^+ , and K^+) where all data for $\Delta G_{\text{latt-3}}$ comes from the NIST webbook except for the ΔH_f of CO_3^{2-} . The ΔH_f of CO_3^{2-} (−128.7 kcal/mol, Supporting Information, Table S10) was calculated at the G4 level with

Table 4. Solvation Free Energies (ΔG_{solv}) of Dianion (CO_3^{2-} , SO_4^{2-} , $\text{C}_8\text{H}_8^{2-}$, and $\text{B}_{12}\text{H}_{12}^{2-}$) with aug-cc-pVTZ Basis Set by Three Different Cavity Sets for CPCM Solvation in kcal/mol at 298.15 K^a

		UFF	UAKS	Pauling
CO_3^{2-}	B3LYP	−244.4(−246.5)	−255.1(−257.4)	−262.9(−265.3)
	PBE	−241.5(−243.9)	−251.7(−254.6)	−258.6(−261.5)
	BVP86	−242.4(−244.7)	−252.8(−255.5)	−259.9(−262.7)
	M05–2X	−248.5(−250.1)	−259.9(−261.6)	−269.0(−271.0)
SO_4^{2-}	B3LYP	−225.6(−227.8)	−234.0(−236.2)	−241.5(−244.2)
	PBE	−223.7(−226.3)	−231.8(−234.4)	−238.5(−241.5)
	BVP86	−224.5(−226.9)	−232.7(−235.2)	−239.7(−242.5)
	M05–2X	−228.4(−230.2)	−237.1(−239.0)	−245.9(−248.2)
$\text{C}_8\text{H}_8^{2-}$	B3LYP	(−186.0)	(−184.2)	(−192.3)
	PBE	(−184.1)	(−182.3)	(−191.4)
	BVP86	(−187.4)	(−184.8)	(−192.8)
	M05–2X	(−192.4)	(−188.6)	(−199.4)
$\text{B}_{12}\text{H}_{12}^{2-}$	B3LYP	−148.1(−147.9)	−139.2(−139.1)	−145.8(−145.7)
	PBE	−147.2(−147.6)	−138.7(−139.5)	−145.9(−145.8)
	BVP86	−147.5(−147.8)	−138.9(−139.5)	−146.3(−146.0)
	M05–2X	−150.2(−150.4)	−140.8(−141.2)	−149.2(−149.0)

^a Values in parentheses are at DFT/6-311++G(3df,2pd).

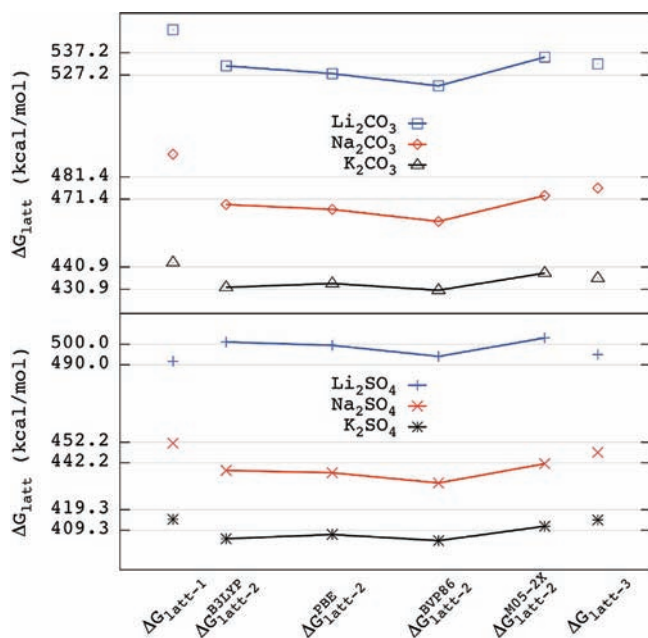


Figure 1. Lattice free energies (ΔG_{latt}) of $M_2\text{CO}_3$ and $M_2\text{SO}_4$ ($M = \text{Li}^+$, Na^+ , and K^+) by three different methods for calculating lattice energies ($\Delta G_{\text{latt-1}} = \text{Jenkins formula}$; $\Delta G_{\text{latt-2}} = \Delta\Delta G + \Delta G_{\text{gas}}$; and $\Delta G_{\text{latt-3}} = \text{Born-Haber cycle}$). Light lines indicate lattice energies ± 5 kcal/mol from the $\Delta G_{\text{latt-3}}$ value.

the isodesmic reaction $\text{SO}_4^{2-} + \text{CO}_2 \rightarrow \text{SO}_3 + \text{CO}_3^{2-}$ and is close to a value reported by Wu and Tiernan⁵⁵ (-124.5 ± 2.3 kcal/mol). The values reported for ΔH_f of CO_3^{2-} in the NIST webbook (-116 ± 10 kcal/mol, average of seven different estimations) is smaller by 12.7 kcal/mol.³⁷ Jenkins et al.⁵⁶ report a value of -76.7 kcal/mol of ΔH_f for CO_3^{2-} using the ΔH_{latt} of CaCO_3 . From the difference in ΔH_f between CO_3^{2-} and CO_3^{2-} , the electron affinity of CO_3^{2-} is -52.0 kcal/mol. When the electron affinity of CO_3^{2-} (calculated at CCSD(T)/aug-cc-pVTZ in a dielectric medium $\epsilon = 100, 50, 25, 10$) is extrapolated to the gas phase ($\epsilon = 1$, Figure 2), a value of -78.2 kcal/mol is obtained. In fact, the gas-phase extrapolated value is the same as the nonextrapolated value (see Figure 2). At the highest levels of theory (CCSD(T)/aug-cc-pV5Z), the electron affinity of CO_3^{2-} becomes -76.8 kcal/mol. For consistency, we used the electron affinity of CO_3^{2-} at the G4 level of theory (-75.5 kcal/mol).

Using an atomization scheme at the G4 level, the values of ΔH_f for gas-phase $M_2\text{CO}_3$ ($M = \text{Li}^+$, Na^+ , and K^+) are -201.0 , -183.4 , and -188.8 kcal/mol, respectively. We computed $\Delta\Delta H_f$ which allowed the determination of $\Delta\Delta G_f$ values (74.8, 73.0, and 71.7 kcal/mol, respectively) with solid ΔH_f . The ΔG_{gas} by the M05-2X functional for $\Delta G_{\text{latt-2}}$ gives the lattice free energy of $M_2\text{CO}_3$ ($M = \text{Li}^+$, Na^+ , and K^+) within ± 5.0 kcal/mol from the $\Delta G_{\text{latt-3}}$ value, whereas $\Delta G_{\text{latt-1}}$ (Jenkins formula) overestimates ΔG_{latt} by 15.3, 15.2, and 7.0 kcal/mol, respectively relative to $\Delta G_{\text{latt-3}}$ (Figure 1).

Figure 3 summarizes $\Delta G_{\text{diss}}^\circ$ of $M_2\text{CO}_3$ ($M = \text{Li}^+$, Na^+ , and K^+) by three different ΔG_{latt} calculation methods combined with $\Delta G_{\text{solv}}(\text{CO}_3^{2-})$ by the Pauling cavity set and $\Delta G_{\text{solv}}(M^+)$ from Kelly et al.³¹ The greatest consistency with experimental $\Delta G_{\text{diss}}^\circ$ values are derived from the M05-2X/Pauling combination, while the UFF and UAKS cavity sets give too positive $\Delta G_{\text{diss}}^\circ$ (Supporting Information, Table S5). The $\Delta G_{\text{diss}}^\circ$ values derived

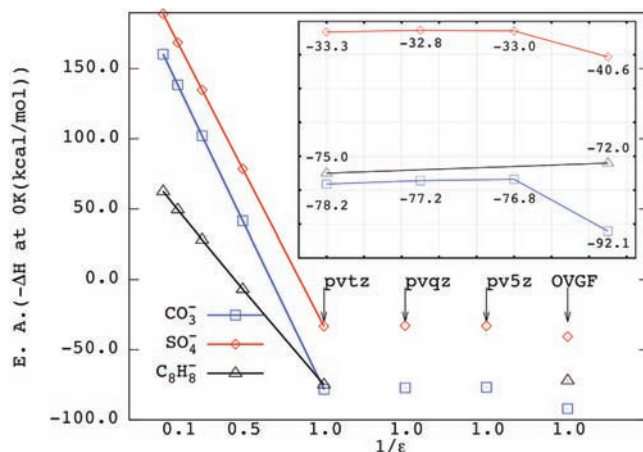


Figure 2. Electron affinity determination ($-\Delta H(0\text{ K})$ for $X^- + e^- \rightarrow X^{2-}$) of CO_3^{2-} , SO_4^{2-} , and C_8H_8^- by three different methods: (1) stabilization by solvation, (2) gas phase using CCSD(T)/aug-cc-pVTZ, and (3) OVGf(P3)/aug-cc-pVQZ for CO_3^{2-} and SO_4^{2-} and OVGf(P3)/6-311+G(3df,2pd) for C_8H_8^- . The geometry of the monoanion is based on B3LYP/GTbas3 (part of G4 level of theory).

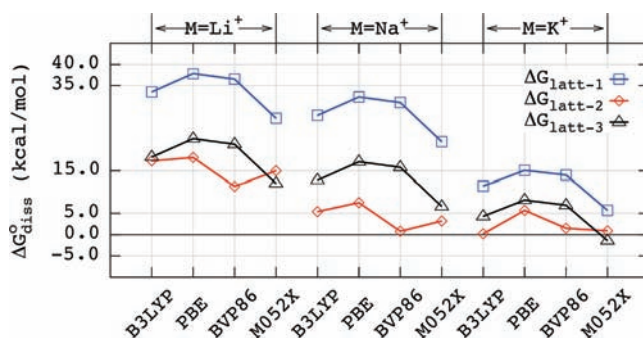


Figure 3. Dissolution free energies ($\Delta G_{\text{diss}}^\circ$) of $M_2\text{CO}_3$ ($M = \text{Li}^+$, Na^+ , and K^+) by three different methods for calculating lattice energies ($\Delta G_{\text{latt-1}} = \text{Jenkins formula}$; $\Delta G_{\text{latt-2}} = \Delta\Delta G + \Delta G_{\text{gas}}$; and $\Delta G_{\text{latt-3}} = \text{Born-Haber cycle}$) combined with the solvation free energy (ΔG_{solv}) of CO_3^{2-} by the Pauling cavity set.

from $\Delta G_{\text{latt-3}}$ and $G_{\text{solv}}(\text{CO}_3^{2-})$ by M05-2X/Pauling differ from $\Delta G_{\text{diss}}^\circ$ with the heat of solution by 7.7, 7.7, and 5.7 kcal/mol, respectively (Table 2 and Supporting Information, Table S5). The M05-2X/Pauling method computes the pK_{a2} of H_2CO_3 to be 14.3 ($\Delta G_{\text{aq}}^2 = 19.3$ kcal/mol) corresponding to an experimental value of 10.3 ($\Delta G_{\text{aq}}^2 = 14.1$ kcal/mol), which corresponds to an underestimation of the $\Delta G_{\text{solv}}(\text{CO}_3^{2-})$ by 5.2 kcal/mol.¹⁰ If this difference is applied to the $\Delta G_{\text{diss}}^\circ$ of $M_2\text{CO}_3$, the difference between experimental $\Delta G_{\text{diss}}^\circ$ and calculated $\Delta G_{\text{diss}}^\circ$ would be 2.5, 2.5, and 0.5 kcal/mol for $M_2\text{CO}_3$ ($M = \text{Li}^+$, Na^+ , and K^+), respectively. The M05-2X functional, which is an improved density functional for dispersion interaction by kinetic energy density,²⁹ gives the best $\Delta G_{\text{diss}}^\circ$ among four DFT functionals.

The instability of $\text{SO}_4^{2-}(\text{g})$ was discussed by several groups.^{19b,57} Zheng et al.²⁰ reported -25.4 kcal/mol for the adiabatic electron affinity of $\text{SO}_4^{2-}(\text{g})$ by an atomization scheme with a MP2/CBS approach. Boldyrev and Simons^{57a} suggested -30.9 kcal/mol for the vertical electron detachment energy of SO_4^{2-} using QCISD(T). In the present work, the G4 level of

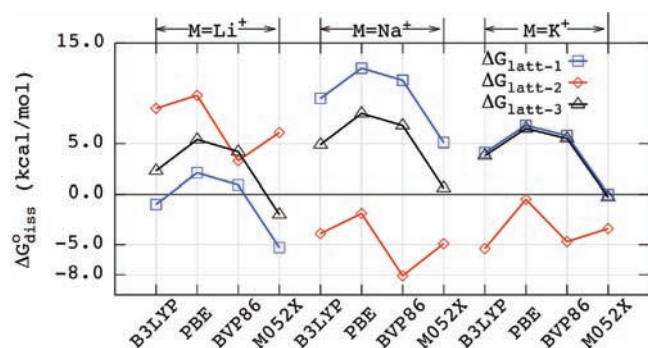


Figure 4. Dissolution free energies ($\Delta G^\circ_{\text{diss}}$) of M_2SO_4 ($\text{M} = \text{Li}^+$, Na^+ , and K^+) by three different methods for calculating lattice energies ($\Delta G_{\text{latt-1}}$ = Jenkins formula; $\Delta G_{\text{latt-2}} = \Delta\Delta G + \Delta G_{\text{gas}}$; and $\Delta G_{\text{latt-3}}$ = Born–Haber cycle) combined with the solvation free energy (ΔG_{solv}) of SO_4^{2-} by the Pauling cavity set.

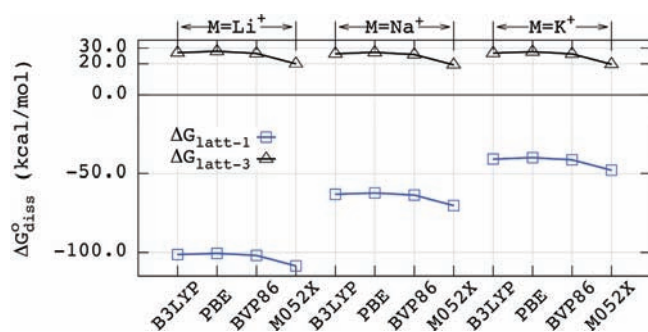
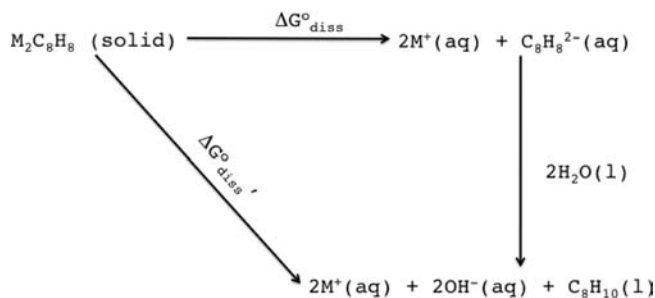


Figure 5. Dissolution free energies ($\Delta G^\circ_{\text{diss}}$) of $\text{M}_2\text{C}_8\text{H}_8$ ($\text{M} = \text{Li}^+$, Na^+ , and K^+) by two different methods for calculating lattice energies ($\Delta G_{\text{latt-1}}$ = Jenkins formula; $\Delta G_{\text{latt-3}}$ = Born–Haber cycle) combined with the solvation free energy (ΔG_{solv}) of $\text{C}_8\text{H}_8^{2-}$ by the Pauling cavity set.

theory gives -32.8 kcal/mol ($\text{SO}_4^- + \text{e}^- \rightarrow \text{SO}_4^{2-}$) while CCSD(T)/aug-cc-pVTZ extrapolated in varying dielectric constants gives -33.3 kcal/mol (Figure 2). At our highest level of theory (CCSD(T)/aug-cc-pV5Z), the electron affinity of SO_4^- becomes -32.8 kcal/mol.

Relative to $\Delta G_{\text{latt-3}}$ values, $\Delta G_{\text{latt-2}}$ underestimates the lattice free energy of Na_2SO_4 and K_2SO_4 but overestimates it for Li_2SO_4 (Figure 1), but in every case, the M05–2X functional is the best DFT choice. For M_2SO_4 ($\text{M} = \text{Li}^+$, Na^+ , and K^+), the Jenkins formula ($\Delta G_{\text{latt-1}}$) is within ± 5.0 kcal/mol of $\Delta G_{\text{latt-3}}$ (Figure 1). For every estimation method of ΔG_{latt} , the M05–2X/Pauling combination yields the best prediction value of $\Delta G^\circ_{\text{diss}}$ for M_2SO_4 ($\text{M} = \text{Li}^+$, Na^+ , and K^+) (Figure 4 and Table 2). To compute $\Delta G_{\text{latt-3}}$ for $\text{M}_2\text{C}_8\text{H}_8$ ($\text{M} = \text{Li}^+$, Na^+ , and K^+), we use ΔH_f° of $\text{Na}_2\text{C}_8\text{H}_8$ (-27.5 kcal/mol) and $\text{K}_2\text{C}_8\text{H}_8$ (-32.0 kcal/mol) from Stevenson et al.^{39a} while ΔH_f° of $\text{Li}_2\text{C}_8\text{H}_8$ (-33.9 kcal/mol) comes from a private communication cited in the NIST webbook.³⁷ The entropy value of $\text{M}_2\text{C}_8\text{H}_8(\text{s})$ is calculated by the Jenkins formula (eq 3).^{22e} For the electron affinity of C_8H_8^- , Dewar et al.⁵⁸ reported -80.9 kcal/mol by the MINDO/2 method while Baik et al.⁵⁹ suggested -79.1 and -85.1 kcal/mol by DFT and Müller et al.⁶⁰ reported -61.6 kcal/mol by G2(MP2). In our computation, CCSD(T)/aug-cc-pVTZ//G4 gives -75.0 kcal/mol (-74.3 kcal/mol by G4 level of theory) while the OVG(P3) approach gives -72.0 kcal/mol

Scheme 5. Dissolution and Protonation Process of $\text{M}_2\text{C}_8\text{H}_8(\text{s}) + 2\text{H}_2\text{O}(\text{l}) \rightarrow 2\text{M}^+(\text{aq}) + 2\text{OH}^-(\text{aq}) + \text{C}_8\text{H}_{10}(\text{l})$ ($\text{M} = \text{Li}^+$, Na^+ , and K^+)



(Figure 2). Dominikowska and Palusiak⁶¹ discussed the stability and aromaticity of $\text{C}_8\text{H}_8^{2-}$ including artifacts caused by using diffuse functions to describe the dianion. Despite the large dianion size, the electron affinity of C_8H_8^- (-74.3 kcal/mol) is similar to that of CO_3^- (-78.2 kcal/mol), which implies that the electronegativity of the atoms is more important than the size of the dianion (Figure 2). Sommerfeld^{19a,62} reports the gas-phase lifetime of $\text{C}_8\text{H}_8^{2-}$ and CO_3^{2-} to be 6 and 6500 fs, respectively.

For the $\Delta G^\circ_{\text{diss}}$ of $\text{M}_2\text{C}_8\text{H}_8$ ($\text{M} = \text{Li}^+$, Na^+ , and K^+), the $\Delta G_{\text{latt-3}}$ and $\Delta G_{\text{solv}}(\text{C}_8\text{H}_8^{2-})$ by the M05–2X/Pauling combination give 20.0, 19.3, and 19.7 kcal/mol, respectively (Figure 5). While the reaction $\text{M}_2\text{C}_8\text{H}_8(\text{s}) \rightarrow 2\text{M}^+(\text{aq}) + \text{C}_8\text{H}_8^{2-}(\text{aq})$ is very non-spontaneous, the protonation of the $\text{C}_8\text{H}_8^{2-}$ can provide additional driving force ($\text{C}_8\text{H}_8^{2-}(\text{aq}) + 2\text{H}_2\text{O}(\text{l}) \rightarrow 2\text{OH}^-(\text{aq}) + \text{C}_8\text{H}_{10}(\text{l})$) (Scheme 5). The overall dissolution free energy ($\Delta G^\circ_{\text{diss}'}$) of $\text{M}_2\text{C}_8\text{H}_8$ at pH 7 ($\text{M}_2\text{C}_8\text{H}_8(\text{s}) + 2\text{H}_2\text{O}(\text{l}) \rightarrow 2\text{M}^+(\text{aq}) + \text{C}_8\text{H}_{10}(\text{l}) + 2\text{OH}^-(\text{aq})$) should be evaluated to explain the dissolution of $\text{M}_2\text{C}_8\text{H}_8(\text{s})$ (Scheme 5). Using M05–2X/6-311++G(3df,2pd) with the CPCM/Pauling cavity set and -264.0 kcal/mol for $\Delta G_{\text{solv}}(\text{H}^+)$, the free energy change $-(\Delta G_{\text{aq}}^1 + \Delta G_{\text{aq}}^2)$ of $2\text{H}^+(\text{aq}) + \text{C}_8\text{H}_8^{2-}(\text{aq}) \rightarrow \text{C}_8\text{H}_{10}(\text{aq})$ is -34.7 kcal/mol at pH 7 (see Supporting Information for details). The overall process $\Delta G^\circ_{\text{diss}'} = \Delta G^\circ_{\text{diss}} - (\Delta G_{\text{aq}}^1 + \Delta G_{\text{aq}}^2)$ is predicted to be spontaneous by -14.7 , -15.4 , and -15.0 kcal/mol for $\text{M}_2\text{C}_8\text{H}_8(\text{s})$, $\text{M} = \text{Li}^+$, Na^+ , K^+ , respectively ($\Delta G_{\text{latt-3}}$ and M05–2X/Pauling).

On the other hand, the $\Delta G_{\text{latt-1}}$ and $\Delta G_{\text{solv}}(\text{C}_8\text{H}_8^{2-})$ by the M05–2X/Pauling combination produces $\Delta G^\circ_{\text{diss}}$ values for $\text{M}_2\text{C}_8\text{H}_8(\text{s}) \rightarrow 2\text{M}^+(\text{aq}) + \text{C}_8\text{H}_8^{2-}(\text{aq})$ that are much too negative (-108.6 , -70.2 , and -47.9 kcal/mol, respectively, Figure 5).^{23a,c} Indeed, Byrd and Rice^{13d} reported that further reoptimization of the Jenkins model would be required to reduce the error in the lattice energies of M_2X_1 or M_2X_2 salts.

While the $\text{M}_2\text{B}_{12}\text{H}_{12}$ salts ($\text{M} = \text{Li}^+$, Na^+ , and K^+) are very stable in the solid and aqueous phase,^{26c,27,63} the experimental heats of formation (ΔH_f°) of the solids are still not known. A previous application of the Jenkins formula used a volume for $\text{B}_{12}\text{H}_{12}^{2-}$ of 0.2390 nm³ that came from the 0.001 au contour of electron density,^{23a} which is slightly smaller than our value of 0.2950 nm³ (Figure 6). However, the small 0.056 nm³ volume difference leads to more than 14.0 kcal/mol of difference in $\Delta G_{\text{latt-1}}$ ($\Delta G^\circ_{\text{diss}}$) of $\text{M}_2\text{B}_{12}\text{H}_{12}$ (Figure 6).

If $\Delta G_{\text{latt-1}}$ is used with the 0.2950 nm³ volume of $\text{B}_{12}\text{H}_{12}^{2-}$, then the $\Delta G^\circ_{\text{diss}}$ values for $\text{M}_2\text{B}_{12}\text{H}_{12}$ ($\text{M} = \text{Li}^+$, Na^+ , and K^+) are computed to be much too spontaneous (-104.7 , -61.4 , and -33.4 kcal/mol, respectively, Supporting Information, Table S8)

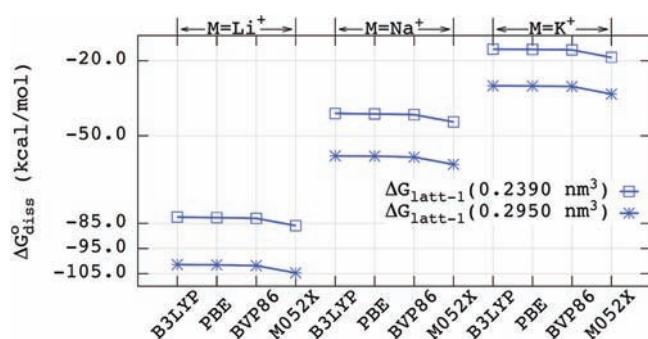


Figure 6. Dissolution free energies ($\Delta G_{\text{diss}}^{\circ}$) of $M_2B_{12}H_{12}$ ($M = \text{Li}^+$, Na^+ , and K^+) by lattice energy estimation of $\Delta G_{\text{latt-1}}^{\circ}$ = Jenkins formula combined with the solvation free energy (ΔG_{solv}) of $B_{12}H_{12}^{2-}$ by the Pauling cavity set.

Table 5. Comparison between Experimental Heats of Formation Differences ($\Delta\Delta H_f$, kcal/mol) and Cohesive Energy (ΔE_{coh} , kcal/mol) by Periodic Boundary Calculation

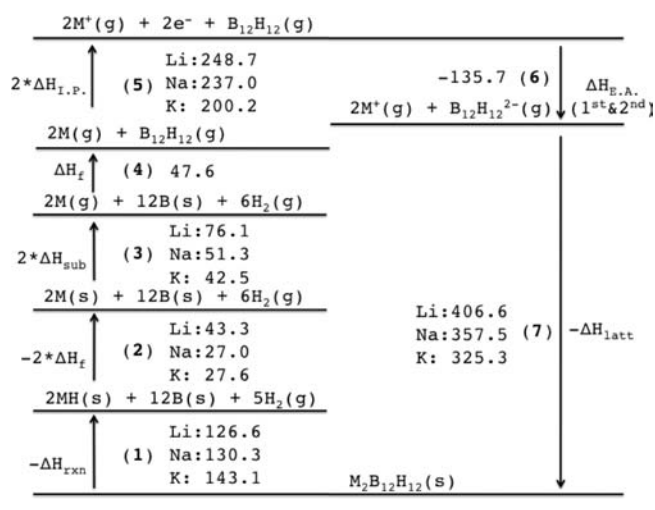
	$\Delta\Delta H_f^a$	$(\Delta E_{\text{coh}} - \Delta\Delta H_f)$				
		BLYP	PBE	PBE-D ^c	PZ	PW91
LiCl	50.8	-10.7	-26.3	-14.3	4.4	-4.3
NaCl	54.9	-11.6	-6.2	4.7	1.1	-4.8
KCl	53.1	6.9	-1.9	5.6	6.9	
Li ₂ SO ₄	94.3	-32.4	-72.1	-55.9	-4.3	-16.5
Na ₂ SO ₄	84.6	-19.4	-6.5	19.1	7.2	-1.9
K ₂ SO ₄	82.1	18.2	6.9	30.8	27.5	
Li ₂ B ₁₂ H ₁₂	61.8 ^b	-33.1	-45.5	-4.7	-1.4	-19.7
Na ₂ B ₁₂ H ₁₂	54.5 ^b	-12.5	-1.5	36.1	18.3	-0.1
K ₂ B ₁₂ H ₁₂	52.0 ^b	56.3	15.1	47.7	35.1	

^aThe difference of ΔH_f between gas and solid state. The values for each salt come from the NIST webbook. ^bThe value is derived by the difference between ΔH_{gas} of $M_2B_{12}H_{12}$ ($M = \text{Li}^+$, Na^+ , and K^+) and presumable lattice enthalpies (ΔH_{latt}) (see text), where $\Delta G_{\text{diss}}^{\circ} = 0$ is arrived with $\Delta G_{\text{solv}}(B_{12}H_{12}^{2-})$ by the Pauling cavity sets. The zero-point and entropy correction are determined from the PM6 semiempirical method with unit cell cluster model of $M_2B_{12}H_{12}$ ($M = \text{Li}^+$, Na^+ , and K^+). ^cDispersion energy correction made by London formula. See ref 11b.

since the experimental values vary between -1.9 to -2.7 kcal/mol (Table 2). Again, the large variation in $\Delta G_{\text{diss}}^{\circ}$ for Li^+ , Na^+ , and K^+ indicates that no single modification of the $B_{12}H_{12}^{2-}$ volume can improve the $\Delta G_{\text{diss}}^{\circ}$ values using the Jenkins formula (Figure 6). Since the experimental ΔH_f values of $M_2B_{12}H_{12}(s)$ ($M = \text{Li}^+$, Na^+ , and K^+) are not available, we could not compute $\Delta G_{\text{latt-2}}^{\circ}$ from $\Delta\Delta H_f$ (between solid and gas). Therefore, we computed $\Delta G_{\text{latt-2}}^{\circ}$ by first computing the cohesion energies ΔE_{coh} from the crystal structures (Table 5).

With $\Delta\Delta H_f$ values from experiment, we first accessed the computed ΔE_{coh} values since $\Delta E_{\text{coh}} = \Delta\Delta H_f - \text{zero-point energies}$. The ΔE_{coh} value for MCl ($M = \text{Li}^+$, Na^+ , and K^+) by BLYP functional underestimates the $\Delta\Delta H_f$ of LiCl and NaCl and overestimates it for KCl. Using the dispersion-corrected PBE functional (PBE-D), the underestimation is adjusted by more than 7.5 kcal/mol for MCl ($M = \text{Li}^+$, Na^+ , and K^+) (Table 5). The PZ and PW91 functionals give a reasonable ΔE_{coh} ($\Delta\Delta H_f$) estimation. However, ΔE_{coh} by every DFT functional underestimates

Scheme 6. Born–Haber Cycle of $M_2B_{12}H_{12}$ ($M = \text{Li}^+$, Na^+ , and K^+) Based on ΔH_{latt} Values Which Makes $\Delta G_{\text{diss}}^{\circ} = 0$



$\Delta\Delta H_f$ of Li_2SO_4 and overestimates $\Delta\Delta H_f$ of K_2SO_4 while ΔE_{coh} of Na_2SO_4 depends on the choice of DFT functional. The best ΔE_{coh} for $M_2\text{SO}_4$ ($M = \text{Li}^+$, Na^+ , and K^+) comes from the PZ, PW91, and PBE functional, respectively. The scaled dispersion corrections for $M_2\text{SO}_4$ ($M = \text{Li}^+$, Na^+ , and K^+) become more than 16.0 kcal/mol (PBE \rightarrow PBE-D). For comparison, the dispersion interaction in the benzene crystal is 13.3 kcal/mol by DFT-D2, 12.0 kcal/mol by symmetry adapted perturbation theory (SAPT), and 10.3 kcal/mol by experiment.^{11fg} Recently, Grimme and co-workers have developed the DFT-D3 method which corrects for the overbinding in the $M^+ \cdot \text{Benzene}$ complex ($M = \text{Li}^+$, Na^+ , and K^+).^{12c} However, the use of DFT-D3 in our system did not produce better results (data is not presented), and Grimme's group is developing values suitable for ionic systems.⁶⁴ It is also possible that the interaction energy of cations and anions is overestimated by DFT methods since it is well-known that DFT exaggerates charge equalization.⁶⁵ In this case, a dispersion correction may possibly appear to "overcorrect" and produce ΔG_{coh} , which are too binding.

To estimate ΔG_{latt} for $M_2B_{12}H_{12}$, we used the M05-2X/Pauling cavity set and assumed that $\Delta G_{\text{diss}}^{\circ} = 0$ (i.e., reversing the process in Scheme 3). The actual $\Delta G_{\text{diss}}^{\circ}$ values for $M_2B_{12}H_{12}$ ($M = \text{Li}^+$, Na^+ , and K^+) by solubility data are slightly negative (Table 2). From ΔG_{latt} we computed ΔH_{latt} by subtracting the ZPE and $T\Delta S$ corrections (406.6, 357.5, and 325.3 kcal/mol, respectively, Scheme 6). We then computed $\Delta\Delta H_f$ by combining ΔH_{latt} and computed gaseous dissociation enthalpies (ΔH_{gas}) of $M_2B_{12}H_{12}$ ($M = \text{Li}^+$, Na^+ , and K^+ ; 344.8, 303.0, and 273.3 kcal/mol, respectively, average of four DFT functionals) (Table 5).

On the basis of these $\Delta\Delta H_f$ values, we find reasonable agreement with the ΔE_{coh} of $\text{Li}_2B_{12}H_{12}$ from the PBE-D and PZ functional (Table 5). For $\text{Na}_2B_{12}H_{12}$, PBE and PW91 give reasonable values of ΔE_{coh} while for $\text{K}_2B_{12}H_{12}$ all functionals calculate values of ΔE_{coh} that are too large. The amount of dispersion correction from PBE to PBE-D for $M_2B_{12}H_{12}$ ($M = \text{Li}^+$, Na^+ , and K^+) is more than 32.0 kcal/mol, and this correction is two times larger than for $M_2\text{SO}_4$ ($M = \text{Li}^+$, Na^+ , and K^+) (Table 5). However, Sedláček et al.⁶⁶ report the binding interaction between benzene and $B_{12}H_{12}^{2-}$ is 11.0 kcal/mol by CCSD(T)/CBS and 9.2 kcal/mol by DFT-SAPT. The DFT-D method uses parameters of the metal atom rather than metal cations, which

may exaggerate cation–cation interactions. On the other hand, dispersion of dianion–dianion interactions may be underestimated.

Determining the ΔH_f of $M_2B_{12}H_{12}$ ($M = Li^+$ and Na^+) is important because this material is an undesirable intermediate in chemical hydrogen storage using alkali metal boranes.^{25d–f,67} On the basis of the predicted crystal structure of $Li_2B_{12}H_{12}$, Ohba et al.⁶⁷ suggested 149.4 kcal/mol for $\Delta H_{rxn}(0\text{ K})$ of $Li_2B_{12}H_{12}(s) \rightarrow 2LiH(s) + 12B(s) + 5H_2(g)$ while Ozolins et al.^{25d} suggest 139.5 kcal/mol for $\Delta H_{rxn}(0\text{ K})$ using a different structure prediction. Scheme 6 presents a Born–Haber cycle of $M_2B_{12}H_{12}$ ($M = Li^+$, Na^+ , and K^+) based on $\Delta G_{diss}^\circ = 0$. Processes 2, 3, and 5 are from the NIST webbook³⁷ while processes 4 and 6 are available from ab initio computations. The Dixon group reported $\Delta H_f(298\text{ K})$ of $B_{12}H_{12}^{2-}$ to be -88.1 kcal/mol with the G3B3 approach, which is the same value as we predict by G4 (-88.1 kcal/mol).^{23a} The value of $\Delta H_{rxn}(1)$ from Scheme 6 for $M_2B_{12}H_{12}$ ($M = Li^+$, Na^+ , and K^+) becomes 126.6, 130.3, and 143.1 kcal/mol, respectively. The difference between our $\Delta H_{rxn}(1)$ and previous reported values for $Li_2B_{12}H_{12}$ are 12.9 kcal/mol^{25d} and 22.8 kcal/mol,⁶⁷ respectively.

Previous work has shown that as the size of the dianion becomes larger, errors in $\Delta H_{rxn}(-\Delta H_f)$ by periodic boundary calculations become larger. For example, Ozolins et al.^{25d} report 14.4 kcal/mol of ΔH_{rxn} for $MgH_2(s) \rightarrow Mg(s) + H_2(g)$ while the NIST webbook data gives 18.2 kcal/mol³⁷ for $-\Delta H_f$ (3.8 kcal/mol difference). By using the PBE functional, Miwa et al.^{25a} reported -38.2 kcal/mol for $\Delta H_f(0\text{ K})$ of $LiBH_4$ while the experimental value is -46.5 kcal/mol⁶⁸ (8.3 kcal/mol difference). When the size of the anion is $B_{12}H_{12}^{2-}$, the difference increases to 56.2 kcal/mol. Specifically, Caputo and Züttel^{25e} reported 226.1 kcal/mol for $-\Delta H_f(0\text{ K})$ of $Li_2B_{12}H_{12}$ from their standard state ($Li_2B_{12}H_{12}(s) \rightarrow 2Li(s) + 12B(s) + 6H_2(g)$) using the experimental crystal structure^{25d} while, the sum of process 1 and 2 (i.e., $-\Delta H_f$ at 298 K) is 169.9 kcal/mol from Scheme 6. Likewise, Caputo et al.^{25f} reported 259.7 kcal/mol for $-\Delta H_f(0\text{ K})$ of $Na_2B_{12}H_{12}$ using the experimental crystal structure which can be compared to 157.3 kcal/mol (i.e., $-\Delta H_f$ at 298 K) for the sum of 1 and 2 from Scheme 6 (102.4 kcal/mol difference). For $K_2B_{12}H_{12}$, our calculations suggest 170.7 kcal/mol for $-\Delta H_f$ at 298 K, which is similar to that of $Li_2B_{12}H_{12}$ (Scheme 6).

CONCLUSIONS

For the calculation of the dissolution Gibbs free energies (ΔG_{diss}°) for M_2X_1 ($M = Li^+$, Na^+ , and K^+ with $X = CO_3^{2-}$, SO_4^{2-} , $C_8H_8^{2-}$, and $B_{12}H_{12}^{2-}$) salts, three methods for ΔG_{latt} estimation are combined with $\Delta G_{solv}(X^{2-})$ by CPCM solvation modeling. The $\Delta G_{solv}(X^{2-})$ by the Pauling cavity set leads to reasonable ΔG_{diss}° values. For small dianions like SO_4^{2-} , the Jenkins formula (ΔG_{latt-1}) provides reliable ΔG_{diss}° values when it is combined with $\Delta G_{solv}(X^{2-})$ by MO5–2X/Pauling cavity sets. However, the thermochemical volume of the dianion is not easily determined by ab initio molecular volume calculations, and the static radii cannot yield reasonable ΔG_{diss}° values when soft (large) dianions are involved. The ΔG_{gas} by ab initio computation followed by $\Delta\Delta G_f$ from literature is useful to determine ΔG_{latt} of salts, but the replacement of $\Delta\Delta G_f$ by ΔG_{coh} greatly depends on the choice of DFT functional in the periodic boundary calculations. When $\Delta G_{diss}^\circ = 0$ is assumed for $M_2B_{12}H_{12}$ ($M = Li^+$, Na^+ , and K^+), our Born–Haber cycle can be used to evaluate solid-state ΔH_f values.

ASSOCIATED CONTENT

S Supporting Information. Thermodynamic values are given for M_1X_1 ($M = Li^+$, Na^+ , and K^+ with $X = F^-$, Cl^- , and Br^-) in Tables S1 and for M_2X_1 ($M = Li^+$, Na^+ , and K^+ with $X = CO_3^{2-}$, SO_4^{2-} , and $B_{12}H_{12}^{2-}$) in Table S2. Table S3 presents ZPE, entropy correction using PM6 method. Table S4 presents ΔG_{latt} by the Jenkins formula. From Table S5 to Table S8, ΔG_{diss}° values of M_2X_1 ($M = Li^+$, Na^+ , and K^+ with $X = CO_3^{2-}$, SO_4^{2-} , $C_8H_8^{2-}$, and $B_{12}H_{12}^{2-}$) are tabulated. Electron affinities of monoanions are given in Table S9 while isodesmic reaction schemes for $M_2CO_3(g)$ ($M = Li^+$, Na^+ , and K^+) are given in Table S10. Table S11 presents ΔE_{coh} calculations. Ab initio computation results with UFF, UAKS, and Pauling cavity sets are summarized in Table S12. Table S13 presents the types of pseudopotential in this study. This material is available free of charge via the Internet at <http://pubs.acs.org>.

AUTHOR INFORMATION

Corresponding Author

*E-mail: mckee@chem.auburn.edu.

ACKNOWLEDGMENT

Computer time was made available on the Alabama Super-computer Network. The authors thank Dr. D. Stanbury, Dr. C. Goldsmith, Dr. S. Grimme, and Dr. K. Patkowski for helpful discussions.

REFERENCES

- (1) Thompson, J. D.; Cramer, C. J.; Truhlar, D. G. *J. Phys. Chem. A* **2004**, *108*, 6532–6542.
- (2) Conway, B. E. *Ionic hydration in chemistry and biophysics*; Elsevier: New York, 1981.
- (3) (a) Franks, F. *Water, a comprehensive treatise*; Plenum Press: New York, 1972. (b) Åqvist, J. *J. Phys. Chem.* **1990**, *94*, 8021–8024. (c) Maye, P. V.; Mezei, M. *THEOCHEM* **1996**, *362*, 317–324. (d) Tissandier, M. D.; Cowen, K. A.; Feng, W. Y.; Gundlach, E.; Cohen, M. H.; Earhart, A. D.; Coe, J. V.; Tuttle, T. R. *J. Phys. Chem. A* **1998**, *102*, 7787–7794. (e) Fawcett, W. R. *J. Phys. Chem. B* **1999**, *103*, 11181–11185. (f) Rempe, S. B.; Pratt, L. R.; Hummer, G.; Kress, J. D.; Martin, R. L.; Redondo, A. *J. Am. Chem. Soc.* **2000**, *122*, 966–967. (g) Zhan, C.-G.; Dixon, D. A. *J. Phys. Chem. A* **2001**, *105*, 11534–11540. (h) Asthagiri, D.; Pratt, L. R.; Ashbaugh, H. S. *J. Chem. Phys.* **2003**, *119*, 2702–2708. (i) Kelly, C. P.; Cramer, C. J.; Truhlar, D. G. *J. Phys. Chem. B* **2006**, *110*, 16066–16081. (j) Jensen, K. P.; Jorgensen, W. L. *J. Chem. Theory Comput.* **2006**, *2*, 1499–1509. (k) Joung, I. S.; Cheatham, T. E. *J. Phys. Chem. B* **2008**, *112*, 9020–9041. (l) Donald, W. A.; Williams, E. R. *J. Phys. Chem. B* **2010**, *114*, 13189–13200. (m) Rempe, S. B.; Asthagiri, D.; Pratt, L. R. *Phys. Chem. Chem. Phys.* **2004**, *6*, 1966–1969. (n) Burgess, J. A. *Metal Ions in Solution*; Ellis Horwood: Chichester, 1978. (o) Noyes, R. M. *J. Am. Chem. Soc.* **1962**, *84*, 513–522. (p) Marcus, Y. *Biophys. Chem.* **1994**, *51*, 111–127. (q) Lamoureux, G.; Roux, B. *J. Phys. Chem. B* **2006**, *110*, 3308–3322. (r) Yu, H.; Whitfield, T. W.; Harder, E.; Lamoureux, G.; Vorobyov, I.; Anisimov, V. M.; MacKerell, A. D., Jr.; Roux, B. *J. Chem. Theory Comput.* **2010**, *6*, 774–786.
- (4) Latimer, W. M. *J. Am. Chem. Soc.* **1926**, *48*, 1234–1239.
- (5) (a) Stefanovich, E. V.; Truong, T. N. *Chem. Phys. Lett.* **1995**, *244*, 65–74. (b) Aguilar, M. A.; Delvalle, F. J. O. *Chem. Phys.* **1989**, *129*, 439–450. (c) Rashin, A. A.; Namboodiri, K. J. *Phys. Chem.* **1987**, *91*, 6003–6012.
- (6) Takano, Y.; Houk, K. N. *J. Chem. Theory Comput.* **2005**, *1*, 70–77.
- (7) Chipman, D. M. *J. Phys. Chem. A* **2002**, *106*, 7413–7422.
- (8) Król, M.; Wrona, M.; Page, C. S.; Bates, P. A. *J. Chem. Theory Comput.* **2006**, *2*, 1520–1529.

- (9) Fernandez, M. I.; Canle, M.; Garcia, M. V.; Santaballa, J. A. *Chem. Phys. Lett.* **2010**, *490*, 159–164.
- (10) Lee, T. B.; McKee, M. L. *Phys. Chem. Chem. Phys.* **2011**, *13*, 10258–10269.
- (11) (a) Nabok, D.; Puschnig, P.; Ambrosch-Draxl, C. *Phys. Rev. B* **2008**, *77*, 245316. (b) Barone, V.; Casarin, M.; Forrer, D.; Pavone, M.; Sambi, M.; Vittadini, A. *J. Comput. Chem.* **2009**, *30*, 934–939. (c) Todorova, T.; Delley, B. *J. Phys. Chem. C* **2010**, *114*, 20523–20530. (d) Tsuzuki, S.; Orita, H.; Honda, K.; Mikami, M. *J. Phys. Chem. B* **2010**, *114*, 6799–6805. (e) Berland, K.; Hyldgaard, P. *J. Chem. Phys.* **2010**, *132*, 134705. (f) Beran, G. J. O.; Nanda, K. *J. Phys. Chem. Lett.* **2010**, *1*, 3480–3487. (g) Bučko, T.; Hafner, J.; Lebègue, S.; Ángyán, J. G. *J. Phys. Chem. A* **2010**, *114*, 11814–11824.
- (12) (a) Grimme, S.; Antony, J.; Schwabe, T.; Muck-Lichtenfeld, C. *Org. Biomol. Chem.* **2007**, *5*, 741–758. (b) Grimme, S. *J. Comput. Chem.* **2006**, *27*, 1787–1799. (c) Grimme, S.; Antony, J.; Ehrlich, S.; Krieg, H. *J. Chem. Phys.* **2010**, *132*, 154104.
- (13) (a) King, C. J. *Chem. Educ.* **2005**, *82*, 1584–1584. (b) Glasser, L.; von Szentpály, L. *J. Am. Chem. Soc.* **2006**, *128*, 12314–12321. (c) von Szentpály, L. *J. Am. Chem. Soc.* **2008**, *130*, 5962–5973. (d) Byrd, E. F. C.; Rice, B. M. *J. Phys. Chem. A* **2009**, *113*, 345–352.
- (14) Stefanovich, E. V.; Boldyrev, A. I.; Truong, T. N.; Simons, J. *J. Phys. Chem. B* **1998**, *102*, 4205–4208.
- (15) (a) von Szentpály, L. *J. Phys. Chem. A* **2010**, *114*, 10891–10896. (b) Cárdenas, C.; Ayers, P.; De Proft, F.; Tozer, D. J.; Geerlings, P. *Phys. Chem. Chem. Phys.* **2011**, *13*, 2285–2293.
- (16) (a) Sablon, N.; De Proft, F.; Geerlings, P.; Tozer, D. J. *Phys. Chem. Chem. Phys.* **2007**, *9*, 5880–5884. (b) Hajgató, B.; De Proft, F.; Szieberth, D.; Tozer, D. J.; Deleuze, M. S.; Geerlings, P.; Nyulászi, L. *Phys. Chem. Chem. Phys.* **2011**, *13*, 1663–1668. (c) Tozer, D. J.; De Proft, F. *J. Chem. Phys.* **2007**, *127*, 034108.
- (17) (a) Puiatti, M.; Vera, D. M. A.; Pierini, A. B. *Phys. Chem. Chem. Phys.* **2009**, *11*, 9013–9024. (b) Puiatti, M.; Vera, D. M. A.; Pierini, A. B. *Phys. Chem. Chem. Phys.* **2008**, *10*, 1394–1399.
- (18) Jensen, F. J. *Chem. Theory Comput.* **2010**, *6*, 2726–2735.
- (19) (a) Sommerfeld, T. *J. Phys. Chem. A* **2000**, *104*, 8806–8813. (b) McKee, M. L. *J. Phys. Chem.* **1996**, *100*, 3473–3481.
- (20) Zheng, W.; Lau, K.-C.; Wong, N.-B.; Li, W.-K. *Chem. Phys. Lett.* **2009**, *467*, 402–406.
- (21) Whitehead, A.; Barrios, R.; Simons, J. *J. Chem. Phys.* **2002**, *116*, 2848–2851.
- (22) (a) Roobottom, H. K.; Jenkins, H. D. B.; Passmore, J.; Glasser, L. *J. Chem. Educ.* **1999**, *76*, 1570–1573. (b) Jenkins, H. D. B.; Roobottom, H. K.; Passmore, J.; Glasser, L. *Inorg. Chem.* **1999**, *38*, 3609–3620. (c) Jenkins, H. D. B.; Glasser, L. *Inorg. Chem.* **2002**, *41*, 4378–4388. (d) Jenkins, H. D. B.; Tudela, D.; Glasser, L. *Inorg. Chem.* **2002**, *41*, 2364–2367. (e) Jenkins, H. D. B.; Glasser, L. *Inorg. Chem.* **2003**, *42*, 8702–8708. (f) Glasser, L.; Jenkins, H. D. B. *Chem. Soc. Rev.* **2005**, *34*, 866–874. (g) Glasser, L.; Jenkins, H. D. B. *J. Chem. Eng. Data* **2011**, *56*, 874–880. (h) Glasser, L.; Jenkins, H. D. B. *Inorg. Chem.* **2008**, *47*, 6195–6202. (i) Jenkins, H. D. B.; Liebman, J. F. *Inorg. Chem.* **2005**, *44*, 6359–6372.
- (23) (a) Nguyen, M. T.; Matus, M. H.; Dixon, D. A. *Inorg. Chem.* **2007**, *46*, 7561–7570. (b) Ishigaki, T.; Nikolic, Z. S.; Watanabe, T.; Matsushita, N.; Yoshimura, M. *Solid State Ionics* **2009**, *180*, 475–479. (c) Geis, V.; Guttsche, K.; Knapp, C.; Scherer, H.; Uzun, R. *Dalton Trans.* **2009**, 2687–2694. (d) Boéré, R. T.; Kacprzak, S.; Keßler, M.; Knapp, C.; Riebau, R.; Riedel, S.; Roemmele, T. L.; Rühle, M.; Scherer, H.; Weber, S. *Angew. Chem., Int. Ed.* **2011**, *50*, 549–552.
- (24) (a) Jenkins, H. D. B.; Thakur, K. P. *J. Chem. Educ.* **1979**, *56*, 576–577. (b) Lide, D. R. *CRC Handbook of Chemistry and Physics*; CRC Press: New York, 2008.
- (25) (a) Miwa, K.; Ohba, N.; Towata, S.; Nakamori, Y.; Orimo, S. *Phys. Rev. B* **2004**, *69*, 245120. (b) Frankcombe, T. J.; Kroes, G. J.; Züttel, A. *Chem. Phys. Lett.* **2005**, *405*, 73–78. (c) Pozzo, M.; Alfè, D. *Phys. Rev. B* **2008**, *77*, 104103. (d) Ozolins, V.; Majzoub, E. H.; Wolverton, C. *J. Am. Chem. Soc.* **2009**, *131*, 230–237. (e) Caputo, R.; Züttel, A. *Mol. Phys.* **2010**, *108*, 1263–1276. (f) Caputo, R.; Garroni, S.; Ollid, D.; Teixidor, F.; Suriñach, S.; Baró, M. D. *Phys. Chem. Chem. Phys.* **2010**, *12*, 15093–15100.
- (26) (a) Patnaik, P. *Handbook of Inorganic Chemicals*; McGraw-Hill: New York, 2002. (b) Linke, W. F.; Seidell, A. *Solubilities of Inorganic and Metal Organic Compounds*; Van Nostrand: New York, 1965. (c) Zhukova, N. A.; Malinina, E. A.; Kuznetsov, N. T. *Zh. Neorg. Khim.* **1985**, *30*, 1292–1294.
- (27) Kuznetsov, N. T.; Klimchuk, G. S. *Russ. J. Inorg. Chem.* **1971**, *16*, 645–648.
- (28) (a) Kanaeva, O. A.; Kuznetsov, N. T.; Sosnovskaya, O. O. *Zh. Neorg. Khim.* **1985**, *26*, 1153–1154. (b) Wen, W. Y.; Chen, C. L. *J. Chem. Eng. Data* **1975**, *20*, 384–387.
- (29) Zhao, Y.; Schultz, N. E.; Truhlar, D. G. *J. Chem. Theory Comput.* **2006**, *2*, 364–382.
- (30) Frisch, M. J.; Trucks, G. W.; Schlegel, H. B.; Scuseria, G. E.; Robb, M. A.; Cheeseman, J. R.; Montgomery, J. J. A.; Vreven, T.; Kudin, K. N.; Burant, J. C.; Millam, J. M.; Iyengar, S. S.; Tomasi, J.; Barone, V.; Mennucci, B.; Cossi, M.; Scalmani, G.; Rega, N.; Petersson, G. A.; Nakatsuji, H.; Hada, M.; Ehara, M.; Toyota, K.; Fukuda, R.; Hasegawa, J.; Ishida, M.; Nakajima, T.; Honda, Y.; Kitao, O.; Nakai, H.; Klene, M.; Li, X.; Knox, J. E.; Hratchian, H. P.; Cross, J. B.; Bakken, V.; Adamo, C.; Jaramillo, J.; Gomperts, R.; Stratmann, R. E.; Yazyev, O.; Austin, A. J.; Cammi, R.; Pomelli, C.; Ochterski, J. W.; Ayala, P. Y.; Morokuma, K.; Voth, G. A.; Salvador, P.; Dannenberg, J. J.; Zakrzewski, V. G.; Dapprich, S.; Daniels, A. D.; Strain, M. C.; Farkas, O.; Malick, D. K.; Rabuck, A. D.; Raghavachari, K.; Foresman, J. B.; Ortiz, J. V.; Cui, Q.; Baboul, A. G.; Clifford, S.; Cioslowski, J.; Stefanov, B. B.; Liu, G.; Liashenko, A.; Piskorz, P.; Komaromi, I.; Martin, R. L.; Fox, D. J.; Keith, T.; Al-Laham, M. A.; Peng, C. Y.; Nanayakkara, A.; Challacombe, M.; Gill, P. M. W.; Johnson, B.; Chen, W.; Wong, M. W.; Gonzalez, C.; Pople, J. A. *Gaussian 03*, Revision E.01; Gaussian, Inc.: Wallingford, CT, 2004.
- (31) Milazzo, G.; Caroli, S.; Sharma, V. K. *Tables of standard electrode potentials*; Wiley: London, 1978.
- (32) (a) Sharpe, P.; Richardson, D. E. *Thermochim. Acta* **1992**, *202*, 173–179. (b) Bartmess, J. E. *J. Phys. Chem.* **1994**, *98*, 6420–6424.
- (33) Cramer, C. J. *Essentials of Computational Chemistry*; John Wiley & Sons: Chichester, 2006.
- (34) Reiss, H.; Heller, A. *J. Phys. Chem.* **1985**, *89*, 4207–4213.
- (35) (a) Donald, W. A.; Leib, R. D.; O'Brien, J. T.; Bush, M. F.; Williams, E. R. *J. Am. Chem. Soc.* **2008**, *130*, 3371–3381. (b) Donald, W. A.; Leib, R. D.; Demireva, M.; O'Brien, J. T.; Prell, J. S.; Williams, E. R. *J. Am. Chem. Soc.* **2009**, *131*, 13328–13337.
- (36) Isse, A. A.; Gennaro, A. *J. Phys. Chem. B* **2010**, *114*, 7894–7899.
- (37) webbook.nist.gov/chemistry, accessed on May 15, 2011.
- (38) Stevenson, G. R.; Valentin, J. *J. Phys. Chem.* **1978**, *82*, 498–500.
- (39) (a) Stevenson, G. R.; Ocasio, I.; Bonilla, A. *J. Am. Chem. Soc.* **1976**, *98*, 5469–5473. (b) Stevenson, G. R.; Zigler, S. S.; Reiter, R. C. *J. Am. Chem. Soc.* **1981**, *103*, 6057–6061.
- (40) Frisch, M. J.; Trucks, G. W.; Schlegel, H. B.; Scuseria, G. E.; Robb, M. A.; Cheeseman, J. R.; Scalmani, G.; Barone, V.; Mennucci, B.; Petersson, G. A.; Nakatsuji, H.; Caricato, M.; Li, X.; Hratchian, H. P.; Izmaylov, A. F.; Bloino, J.; Zheng, G.; Sonnenberg, J. L.; Hada, M.; Ehara, M.; Toyota, K.; Fukuda, R.; Hasegawa, J.; Ishida, M.; Nakajima, T.; Honda, Y.; Kitao, O.; Nakai, H.; Vreven, T.; Montgomery, J. J. A.; Peralta, J. E.; Ogliaro, F.; Bearpark, M.; Heyd, J. J.; Brothers, E.; Kudin, K. N.; Staroverov, V. N.; Keith, T.; Kobayashi, R.; Normand, J.; Raghavachari, K.; Rendell, A.; Burant, J. C.; Iyengar, S. S.; Tomasi, J.; Cossi, M.; Rega, N.; Millam, J. M.; Klene, M.; Knox, J. E.; Cross, J. B.; Bakken, V.; Adamo, C.; Jaramillo, J.; Gomperts, R.; Stratmann, R. E.; Yazyev, O.; Austin, A. J.; Cammi, R.; Pomelli, C.; Ochterski, J. W.; Martin, R. L.; Morokuma, K.; Zakrzewski, V. G.; Voth, G. A.; Salvador, P.; Dannenberg, J. J.; Dapprich, S.; Daniels, A. D.; Farkas, O.; Foresman, J. B.; Ortiz, J. V.; Cioslowski, J.; Fox, D. J. *Gaussian 09*, Revision A.02; Gaussian, Inc.: Wallingford, CT, 2009.
- (41) (a) Cheung, Y. S.; Wong, C. K.; Li, W. K. *THEOCHEM* **1998**, *454*, 17–24. (b) Cheung, T. S.; Law, C. K.; Li, W. K. *THEOCHEM* **2001**, *572*, 243–247.

- (42) (a) Tian, S. X. *J. Phys. Chem. A* **2005**, *109*, 5471–5480. (b) Hopper, H.; Lococo, M.; Dolgounitcheva, O.; Zakrzewski, V. G.; Ortiz, J. V. *J. Am. Chem. Soc.* **2000**, *122*, 12813–12818.
- (43) (a) Nicolaides, A.; Rauk, A.; Glukhovtsev, M. N.; Radom, L. *J. Phys. Chem.* **1996**, *100*, 17460–17464. (b) Cheng, M. F.; Ho, H. O.; Lam, C. S.; Li, W. K. *Chem. Phys. Lett.* **2002**, *356*, 109–119.
- (44) Ramondo, F.; Bencivenni, L. *J. Mol. Struct.* **1990**, *221*, 169–174.
- (45) Bach, A.; Fischer, D.; Jansen, M. *Z. Anorg. Allg. Chem.* **2009**, *635*, 2406–2409.
- (46) (a) Alcock, N. W.; Evans, D. A.; Jenkins, H. D. B. *Acta Crystallogr., Sect. B* **1973**, *29*, 360–361. (b) Nord, A. G. *Acta Chem. Scand.* **1973**, *27*, 814–822. (c) McGinnety, J. A. *Acta Crystallogr., Sect. B* **1972**, *28*, 2845–2852.
- (47) Dubbeldam, G. C.; Dewolff, P. M. *Acta Crystallogr., Sect. B* **1969**, *25*, 2665–2667.
- (48) (a) Noordik, J. H.; Vandenha, T.; Mooij, J. J.; Klaassen, A. A. *Acta Crystallogr., Sect. B* **1974**, *30*, 833–835. (b) Hu, N. H.; Gong, L. X.; Jin, Z. S.; Chen, W. Q. *J. Organomet. Chem.* **1988**, *352*, 61–66.
- (49) (a) Her, J. H.; Yousufuddin, M.; Zhou, W.; Jalisatgi, S. S.; Kulleck, J. G.; Zan, J. A.; Hwang, S. J.; Bowman, R. C.; Udovic, T. J. *Inorg. Chem.* **2008**, *47*, 9757–9759. (b) Her, J. H.; Zhou, W.; Stavila, V.; Brown, C. M.; Udovic, T. J. *J. Phys. Chem. C* **2009**, *113*, 11187–11189. (c) Tiritiris, I.; Schleid, T. *Z. Anorg. Allg. Chem.* **2003**, *629*, 1390–1402. (d) Yousufuddin, M.; Her, J. H.; Zhou, W.; Jalisatgi, S. S.; Udovic, T. J. *Inorg. Chim. Acta* **2009**, *362*, 3155–3158.
- (50) Giannozzi, P.; Baroni, S.; Bonini, N.; Calandra, M.; Car, R.; Cavazzoni, C.; Ceresoli, D.; Chiarotti, G. L.; Cococcioni, M.; Dabo, I.; Dal Corso, A.; de Gironcoli, S.; Fabris, S.; Fratesi, G.; Gebauer, R.; Gerstmann, U.; Gougoussis, C.; Kokalj, A.; Lazzeri, M.; Martin-Samos, L.; Marzari, N.; Mauri, F.; Mazzarello, R.; Paolini, S.; Pasquarello, A.; Paulatto, L.; Sbraccia, C.; Scandolo, S.; Sclauzero, G.; Seitsonen, A. P.; Smogunov, A.; Umari, P.; Wentzcovitch, R. M. *J. Phys.: Condens. Matter* **2009**, *21*, 395502.
- (51) MOPAC2009; openmopac.net/home.html, accessed on 3/31/2011.
- (52) Sherwood, P. M. A. *Vibrational spectroscopy of solids*; Cambridge University Press: London, 1972.
- (53) (a) Calle-Vallejo, F.; Martínez, J. I.; García-Lastra, J. M.; Mogensen, M.; Rossmeisl, J. *Angew. Chem., Int. Ed.* **2010**, *49*, 7699–7701. (b) Martínez, J. I.; Hansen, H. A.; Rossmeisl, J.; Nørskov, J. K. *Phys. Rev. B* **2009**, *79*, 045120.
- (54) (a) Jenkins, H. D. B. *J. Chem. Educ.* **2005**, *82*, 950–952. (b) Gavezzotti, A. *Mod. Sim. Mat. Sci. Eng.* **2002**, *10*, 1–29. (c) Giacovazzo, C. *Fundamentals of Crystallography*; Oxford University Press: New York, 2002.
- (55) Wu, R. L. C.; Tiernan, T. O. *Planet. Space Sci.* **1981**, *29*, 735–739.
- (56) Jenkins, H. D. B.; Pratt, K. F.; Smith, B. T.; Waddington, T. C. *J. Inorg. Nucl. Chem.* **1976**, *38*, 371–377.
- (57) (a) Boldyrev, A. I.; Simons, J. *J. Phys. Chem.* **1994**, *98*, 2298–2300. (b) Blades, A. T.; Kebarle, P. *J. Am. Chem. Soc.* **1994**, *116*, 10761–10766.
- (58) Dewar, M. J. S.; Harget, A.; Haselbach, E. *J. Am. Chem. Soc.* **1969**, *91*, 7521–7523.
- (59) Baik, M. H.; Schauer, C. K.; Ziegler, T. *J. Am. Chem. Soc.* **2002**, *124*, 11167–11181.
- (60) Miller, T. M.; Viggiano, A. A.; Miller, A. E. S. *J. Phys. Chem. A* **2002**, *106*, 10200–10204.
- (61) (a) Dominikowska, J.; Palusiak, M. *New J. Chem.* **2010**, *34*, 1855–1861. (b) Dominikowska, J.; Palusiak, M. *J. Comput. Chem.* **2011**, *32*, 1441.
- (62) Sommerfeld, T. *J. Am. Chem. Soc.* **2002**, *124*, 1119–1124.
- (63) McKee, M. L.; Wang, Z. X.; Schleyer, P. v. R. *J. Am. Chem. Soc.* **2000**, *122*, 4781–4793.
- (64) personal communication with Prof. Stefan Grimme.
- (65) Bally, T.; Sastry, G. N. *J. Phys. Chem. A* **1997**, *101*, 7923–7925.
- (66) Sedláč, R.; Fanfrlík, J.; Hnyk, D.; Hobza, P.; Lepšík, M. *J. Phys. Chem. A* **2010**, *114*, 11304–11311.
- (67) Ohba, N.; Miwa, K.; Aoki, M.; Noritake, T.; Towata, S.; Nakamori, Y.; Orimo, S.; Züttel, A. *Phys. Rev. B* **2006**, *74*, 075110.
- (68) Züttel, A.; Wenger, P.; Rentsch, S.; Sudan, P.; Mauron, P.; Emmenegger, C. *J. Power Sources* **2003**, *118*, 1–7.